Tectonophysics 609 (2013) 331–352

Contents lists available at ScienceDirect

Tectonophysics

journal homepage: www.elsevier.com/locate/tecto

Review Article

The lunar moho and the internal structure of the Moon: A geophysical perspective

A. Khan [a,*], A. Pommier [b], G.A. Neumann [c], K. Mosegaard [d]

[a] Institute of Geochemistry and Petrology, Swiss Federal Institute of Technology, Zürich, Switzerland
[b] School of Earth and Space Exploration, Arizona State University, Tempe, USA
[c] NASA Goddard Space Flight Center, Greenbelt, MD, USA
[d] Department of Informatics and Mathematical Modelling, Technical University of Denmark, Lyngby, Denmark

ARTICLE INFO

Article history:
Received 2 May 2012
Received in revised form 7 February 2013
Accepted 14 February 2013
Available online 24 February 2013

Keywords:
Lunar seismology
Crustal thickness
Lunar structure and composition
Lunar gravity and topography
Lunar origin and evolution

ABSTRACT

Extraterrestrial seismology saw its advent with the deployment of seismometers during the Apollo missions that were undertaken from July 1969 to December 1972. The Apollo lunar seismic data constitute a unique resource being the only seismic data set which can be used to infer the interior structure of a planetary body besides the Earth. On-going analysis and interpretation of the seismic data continues to provide constraints that help refine lunar origin and evolution. In addition to this, lateral variations in crustal thickness (~0–80 km) are being mapped out at increasing resolution from gravity and topography data that have and continue to be collected with a series of recent lunar orbiter missions. Many of these also carry onboard multi-spectral imaging equipment that is able to map out major-element concentration and surface mineralogy to high precision. These results coupled with improved laboratory-based petrological studies of lunar samples provide important constraints on models for lunar magma ocean evolution, which ultimately determines internal structure. Whereas existing constraints on initial depth of melting and differentiation from quantitative modeling suggested only partial Moon involvement (<500 km depth), more recent models tend to favor a completely molten Moon, although the former cannot be ruled out sensu stricto. Recent geophysical analysis coupled with thermodynamical computations of phase equilibria and physical properties of mantle minerals suggest that the Earth and Moon are compositionally distinct. Continued analysis of ground-based laser ranging data and recent discovery of possible core reflected phases in the Apollo lunar seismic data strengthens the case for a small dense lunar core with a radius of <400 km corresponding to 1–3% of lunar mass.

Contents

* Corresponding author. Tel.: +41 633442626; fax: +41 446331065.
E-mail address: amir.khan@erdw.ethz.ch (A. Khan).

0040-1951/$ – see front matter © 2013 Elsevier B.V. All rights reserved.
http://dx.doi.org/10.1016/j.tecto.2013.02.024

1. Introduction

Our current view and understanding of the lunar interior has been shaped to a large extent from knowledge and data acquired during and after the Apollo missions and continues up to this day. Through analysis of returned samples, data from surface-deployed experiments, and remote sensing the Apollo program of the late 60s and early 70s did much to advance our understanding of the formation and evolution of the Moon and inner solar system. In spite of the cornucopia of new information about the solar system that has been unwielded by space exploration in the last four decades it has proved difficult to hypothesize on the origin of the solar system or even the Moon until comparatively recently, given the complexity in having to assimilate a vast amount of data from differing fields. In pre-Apollo times it was commonly believed that the Moon compared to Earth is geologically an inactive planet and exactly for that reason it might contain the important evidence that would unravel the mysteries of the solar system and settle the question of its origin, providing the justification for the manned lunar missions. The Moon turned out to be highly differentiated, preserving a record of earliest igneous activity and geochemical fractionation in a small planet. After return of the first lunar samples crucial information on ages, chemistry and the significance of cratering was provided. The evidence from the observed wide range of impact crater sizes led to the notion that a hierarchy of objects existed during accretion, and that the planets accreted from these rather than from dust as initially assumed.

Of all geophysical methods used to study a planet's structure, seismology is uniquely suited to determine many parameters that are critically important to understanding its dynamic behavior and for this reason has played a leading role in the study of Earth's interior. As described in more detail in e.g., Lognonné and Johnson (2007) and Neal (2009) extraterrestrial seismology saw its beginning with the decision to study the Moon seismically in 1959 with the Ranger program, which was designed to land an instrumentation package on the lunar surface. The Ranger seismometer consisted of a single-axis (vertical component) seismometer, but was abandoned after three unsuccessful attempts. With the Surveyor soft lunar landing missions, in the mid-60s, another opportunity presented itself. However, due to decreased payload capabilities and a change of goals by mission planners no seismometer was deployed. Only with the Apollo program did a seismic network on the lunar surface materialize. Although information concerning the seismicity of other bodies in the solar system is limited, seismic observations on Mars and Venus have also been undertaken (e.g., Anderson et al., 1977; Ksanfomality et al., 1982).

The origin of Earth's Moon has been a long-standing problem not without its false leads dating back to the times of Darwin. It has also figured in tales where the Moon is regarded as a somewhat unique object being made of material only known to man on Earth and early measurements on returned Apollo samples did not entirely dispel this hypothesis as is evidenced below in Table 1.

Our general picture of the interior of the Moon and a lot of the concepts that are an ingrained part of lunar science today were conceived as a direct result of data analysis derived from the Apollo missions in the form of remote sensing, surface exploration and sample return. For example, geochemical and petrological studies of returned samples led to the notion of a low-density lunar crust consisting of anorthosite that is believed to have originated by crystallization and subsequent flotation in a magma ocean (e.g., Warren, 1985). This concept of an initially molten Moon has come to constitute the framework for understanding lunar evolution and many of the predicted outcomes of this model are in principle amenable to geophysical investigation. This includes, but is not limited to, questions regarding initial depth of melting of the Moon in order to produce the plagioclase-rich highland crust and possible presence of other deeper-lying mantle compositional/seismic discontinuities. Also within the realm of geophysical testability is the question of compositional kinship between Earth and Moon. While a consensus surrounding lunar formation has emerged, tying its origin to a major collisional episode with Earth about 4.5 Gyr ago (Halliday et al., 2000) from the debris produced when a Mars-sized planetesimal collided with proto-Earth (e.g., Cameron, 2000; Cameron and Benz, 1991; Canup, 2004; Canup and Asphaug, 2001), there is less agreement on the compositional relationship of Earth and Moon (e.g., Khan et al., 2006a; Kuskov and Kronrod, 2009; Kuskov et al., 2002; Pahlevan et al., 2011; Ringwood, 1977; Taylor, 1982; Taylor et al., 2006; Warren, 1986, 2005; Warren and Rasmussen, 1987).

With emphasis on lunar geophysics, and seismology in particular, the purpose of this study is to provide a review of our current state of knowledge of the lunar interior, particularly the crust–mantle interface, the Mohorovičić discontinuity (hereinafter referred to simply as Moho). However, as our knowledge of the "lunar seismic Moho" is limited because of paucity of seismic data, which only provide a very localized picture, gravity and topography data from a host of previous and current missions (see below) will be summarized briefly as these have the means of "filling the gap" and enabling a planet-wide view of the crust–mantle interface. Moreover, as our views have had to be corrected and refined from what we learned from remote sensing missions undertaken in the 90s (Galileo, Clementine, Lunar Prospector) and current lunar orbiter missions (e.g., SMART-1, SELENE, Chandrayaan-1, Chang'E-1, Lunar Reconnaissance Orbiter) as well as analysis of old and new lunar meteorites and samples, a slightly broader scope will be presented here in an attempt to provide a short synthesis between geophysical, petrological and geochemical results. Ultimately, as the nature of the lunar Moho is intimately linked to the evolution of the deep lunar interior, this review will provide an overview of the latter also with the focus centered on the evidence provided by seismology.

The present review is by no means thought to be exhaustive and the review on the lunar interior structure by Wieczorek et al. (2006), including the accompanying set of reviews, published in *New Views of*

Table 1
Seismic velocities in selected cheeses, lunar and terrestrial rocks.
Adapted from Schreiber and Anderson (1970).

	P-wave velocity (km/s)
Cheeses & Sapsego (Swiss)	2.12
Romano (Italy)	1.74
Cheddar (Vermont)	1.72
Muenster (Wisconsin)	1.57
Lunar rocks & Basalt 10017	1.84
Basalt 10046	1.25
Near-surface layer	1.2
Terrestrial rocks & Granite	5.9
Gneiss	4.9
Basalt	5.8
Sandstone	4.9

the Moon (Jolliff et al., 2006) is, although not entirely up-to-date, probably the most comprehensive currently available. Not all aspects of lunar geophysics will be covered here and the interested reader is referred to the above or other more specialized reviews. Of general interest are the lunar geophysics reviews of Hood (1986) and Hood and Zuber (2000), while lunar and planetary seismology is further reviewed by e.g., Lognonné (2005) and Lognonné and Johnson (2007).

2. Lunar seismology—a resumé of past and present investigations

2.1. The Apollo lunar seismic network

The Moon is the only body besides the Earth for which we have seismic data to deduce its internal structure. Lunar seismology saw its beginning with the landing of Apollo 11 in the southwestern part of Mare Tranquilitatis in July 1969 (Fig. 1) and continued on subsequent missions culminating with the landing of Apollo 17 in December 1972. As part of the Apollo Lunar Surface Experiment Package (ALSEP), which consisted of an integrated set of geophysical experiments, a seismometer was deployed during each of the Apollo missions (Fig. 2) except for Apollo 17, which was designed to carry a gravimeter.

Each seismometer consisted of a three-component long-period (bandwidth 1–15 s) and a short-period sensor unit (bandwith 0.125–1 s), which was sensitive to vertical motion at higher frequencies (for instrumental details see Latham et al. (1969)). With the exception of the Apollo 11 seismometer, which was only operative for one lunation, the other four seismometers (powered by radioisotope thermoelectric generators) functioned simultaneously as a seismic array transmitting data continuously from April 1972 until transmission of seismic data was suspended in September 1977 (Apollo-era processing of seismic data is described in Nakamura et al., 1980).

The four-station lunar seismic network spans a relatively small area on the near face of the Moon and is arranged approximately in an equilateral triangle configuration with Apollo stations 12, 15 and 16 placed ~1100 km apart, whereas Apollo stations 12 and 14 were placed in one corner 180 km apart (see Fig. 2).

In the >8 yrs of operation more than 12,000 events were recorded and catalogued (Nakamura et al., 1981), although a large number of these could not be classified. As a result of increased computational resources since Apollo-times this work has continued (Bulow et al., 2005; Nakamura, 2003, 2005) and is yet to be completed. Identified events are summarized in Table 2. Most of the moonquakes are very small with equivalent body-wave magnitudes around 1–3 in case of the deep moonquakes, while ranging up to 5 for a set of shallow events (Goins et al., 1981a). However, because of the high sensitivity of the seismometers and the low level of microseismic background noise (the latter was not resolvable) each station detected on average in the range of 650–1250 moonquakes per year. In comparison to Earth lunar seismic energy release is several orders of magnitude less, ranging from ~10^{10}–10^{14} J/yr compared to 10^{18} J/yr by earthquakes (Goins et al., 1981a; Nakamura, 1980).

Examining the first lunar seismic data in 1969 turned out to be somewhat of a surprise owing to an apparent complexity inherent in lunar seismograms not usually encountered in terrestrial counterparts (this is clearly brought out when studying some of the earliest reports on interpretation of the lunar seismic signals e.g., Latham et al., 1970a, 1970b, 1971). Lunar seismic signals were typically of very long duration, of high frequency, and of reverberating nature with small first arrivals and slowly building amplitudes followed by a slow decay

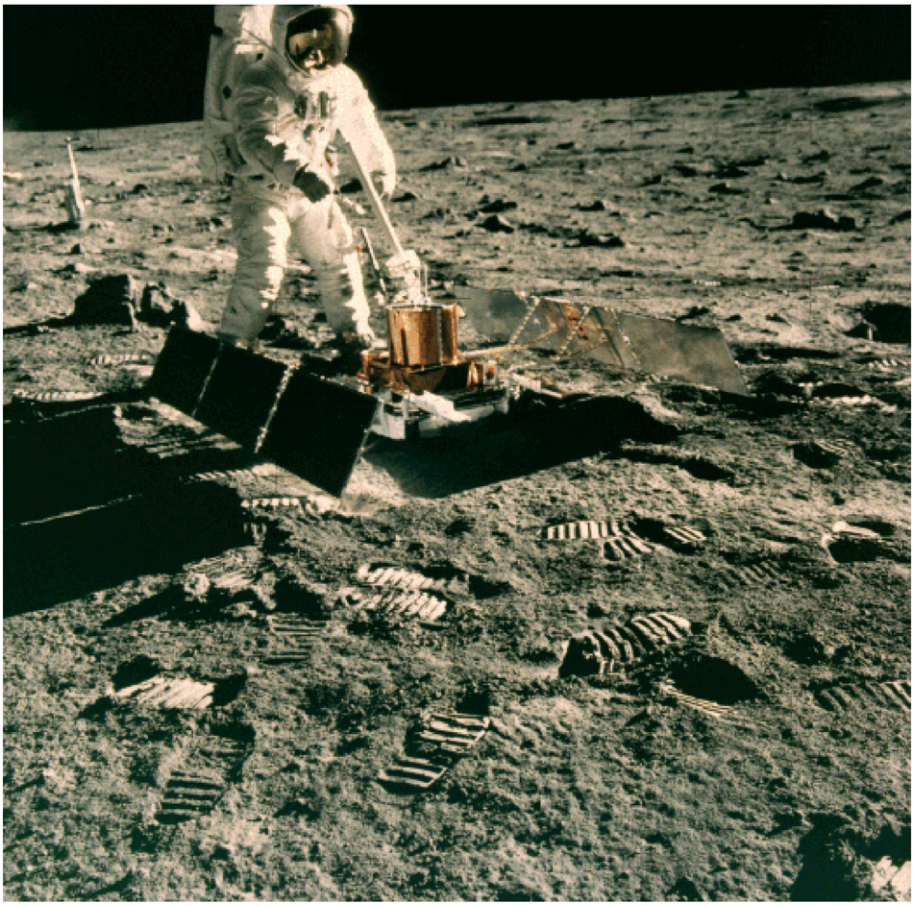

Fig. 1. Deployment of the seismometer during the Apollo 11 mission (AS11-40-5951 courtesy of NASA).

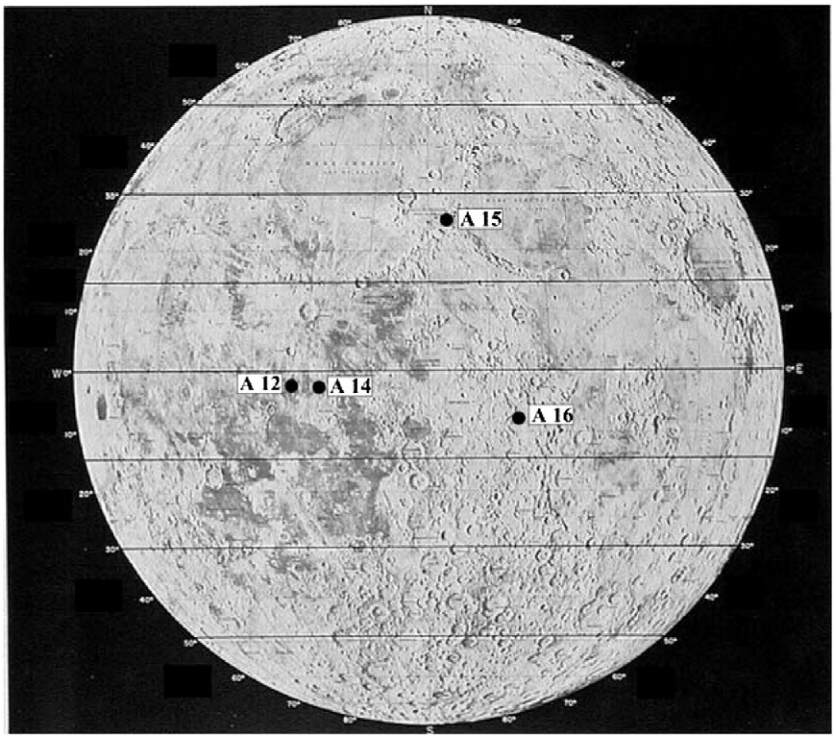

Fig. 2. Front side of the Moon showing locations of the four Apollo lunar seismic stations that operated simultaneously. Distances between stations A12, A15 and A16 are ~1100 km, whereas stations A12 and A14 are 180 km apart. Used by permission of the American Geophysical Union, from Khan and Mosegaard (2002), Journal of Geophysical Research, Vol. 107, Fig. 1, p. 20.

(Latham et al., 1972). Unlike the Earth, where the main seismic pulses in general are of rather short duration, the most prominent feature of lunar signals is their anomalous long continuance (Fig. 3). For example, strong signals from the impacts of the upper stage of the Saturn rocket last several hours. Moonquake and meteoroid impact signals typically continue for 30 min to 2 h (Lammlein et al., 1974). After the first one or two cycles of the P-wave, ground motion is very complex, with no apparent correlation between any two components, obscuring identification of any secondary phases in the coda. It has been suggested that these signals are caused by intense scattering of the waves in the uppermost layers of the lunar crust (e.g., Latham et al., 1972; Nakamura, 1977a). Topographic features, lunar regolith, compositional boundaries, and especially joints and cracks in the crust become very efficient scatterers in the absence of water and volatiles and thus absence of damping (Lammlein et al., 1974; Latham et al., 1972; Toksöz et al., 1974).

2.2. Moonquake variety

Four distinct types of events have been identified and classified according to their signal characteristics: deep moonquakes, shallow moonquakes, and thermal moonquakes, which reflect the present dynamic state of the lunar interior, and meteoroid impacts (see Fig. 3). Seismograms from moonquakes, for example, showed strong S-wave arrivals and indistinct P-wave arrivals, while the reverse was the case for meteoroid impacts.

Table 2
Catalogued events. From Nakamura et al. (1982) and the most recent event catalog (levent.1008). This catalog, with accompanying explanation of entries (EvCatEntries.1008), is available from the public ftp site: ftp.ig.utexas.edu/pub/PSE/catsrepts. For completeness it should be noted that an additional 555 events not accounted for here are contained in the latest event catalog.

Type	Number of events (1982)	Number of events (present)
Artificial impacts	9	9
Meteoroid impacts	1743	1744
Shallow moonquakes	28	28
Deep moonquakes	3145	7083
Unclassified	7633	3639

2.2.1. Deep moonquakes

The most numerous events, the deep moonquakes, were found to be located halfway toward the center of the Moon in the depth range of 700–1200 km (Nakamura, 2005; Nakamura et al., 1982). They consist of repetitive moonquakes that emanate from specific source regions or nests about a kilometer in diameter that are fixed in space (Nakamura, 1978). This results in many nearly identical wave trains and allows summing a large number of moonquake signals to improve signal-to-noise ratio. At most hypocenters, one moonquake occurred for a period of a few days during a fixed time in the monthly lunar tidal cycle, giving rise to peaks at 27-day intervals of the observed lunar seismic activity (Lammlein, 1977; Lammlein et al., 1974; Nakamura, 2005). In addition, a 206-day variation and a 6-year variation in the activity, also due to tidal effects, such as the solar perturbation of the lunar orbit, have been observed (Lammlein, 1977; Lammlein et al., 1974). These observations suggested that the deep moonquakes are related to the tidal forces acting on the Moon (Cheng and Toksöz, 1978; Koyama and Nakamura, 1980; Minshull and Goulty, 1988; Nakamura, 1978; Toksöz et al., 1977). Recent work focusing on the relation of deep moonquake activity with orbital parameters (e.g., Bulow et al., 2007) has showed that activity correlates with the lunar monthly phases (Nakamura, 2005) and orbital eccentricity (Weber et al., 2009). The exact cause of deep moonquakes remains enigmatic though, but may turn out to be related to the presence of fluids, particularly water, (Saal et al., 2008) and/or partial melt and thus to the manner in which some earthquakes occur (Frohlich and Nakamura, 2009). However, the implications of dehydration or melting processes in the lunar interior are poorly constrained.

The 3000+ events were initially found to belong to 109 distinct deep moonquake hypocenters (Nakamura et al., 1982) based on visual matching of signals, all but one of which were located on the nearside.

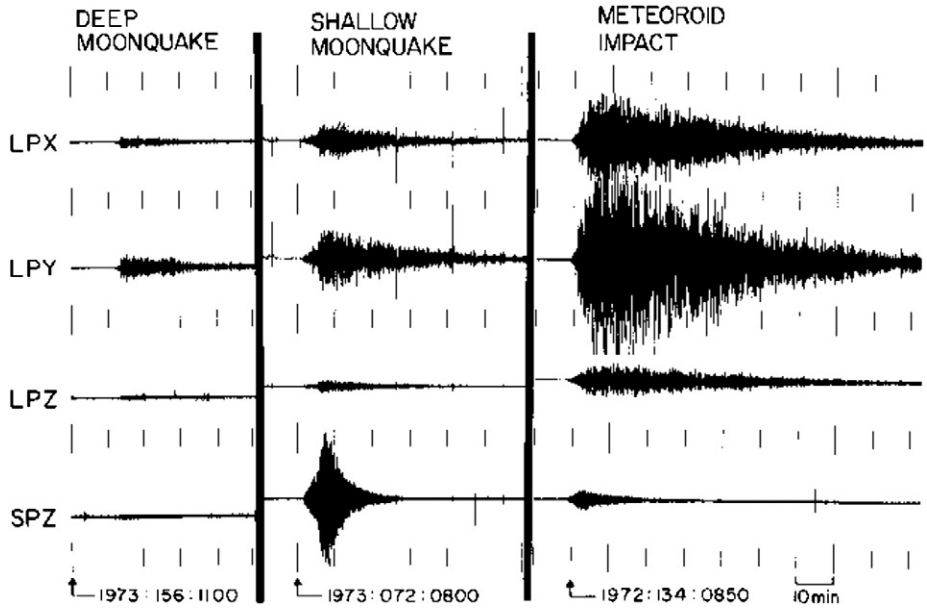

Fig. 3. Summary of lunar seismograms in compressed time scale indicative of the different types of lunar seismicity (signals from thermal moonquakes are not included) as recorded at Apollo station 16. LPX, LPY, LPZ, and SPZ denote long-period components (two horizontal X and Y and one vertical Z), and short-period vertical component, respectively. From Nakamura et al. (1974b).

A recent and presently ongoing campaign to search the unclassified events for other deep moonquakes using correlation of seismic waveforms have helped increase the number of distinct deep moonquake nests to 316 (Nakamura, 2003, 2005). Comparison of identified events then and now (Table 2) clearly highlights the importance of modern-day computing techniques in handling such large data sets.

Of all located deep moonquake clusters to date none are found to occur within ~40° of the antipode of the Moon (Nakamura, 2005), signaling that moonquakes are either absent in this region or that seismic waves do not penetrate the central parts due to presence of partial melt and/or liquid (Nakamura et al., 1973; Weber et al., 2010), thereby limiting the depth to which the interior of the Moon can be sensed by seismic waves.

2.2.2. Shallow moonquakes

Shallow moonquakes are the most energetic and the least frequent lunar seismic sources observed to date with an average of 4 events per year (Nakamura, 1977b). Compared to the deep moonquakes they are relatively strong with an equivalent body-wave magnitude of around 3 and as high as 5.5 (Goins et al., 1981a). Also known as high-frequency-teleseismic (HFT) events owing to their unusually high frequency content (clearly visible on the short-period component in Fig. 3) and the great distances at which they were observed (Nakamura et al., 1974a), estimation of source depth at which they occur has been inconclusive, although there is evidence that they occur in the upper mantle in the depth range of 50–220 km (Khan et al., 2000). This is in line with other evidence, such as the variation of the observed amplitude of HFT signals with distance, which suggests that they originated no deeper than a few hundred kilometers (Nakamura et al., 1979). No clear correlation between shallow moonquakes and the tides has been observed (Nakamura, 1977b), suggesting a possible tectonic origin considering their similarity to intraplate earthquakes (Nakamura, 1980). Their mechanism, though, could not be explained by plate motion, because of a lack of concentration of events into narrow belts as observed on Earth. An alternative suggestion has been advanced by Frohlich and Nakamura (2006) and Banerdt et al. (2006), who investigated the possibility that shallow moonquakes may instead be triggered by objects emanating from outside the solar system, such as nuggets of strange quark matter. However, given the limited number of shallow moonquakes observed to date (28), the statistical significance of this conclusion will most likely have to await the acquisition of new lunar seismic data.

2.2.3. Thermal moonquakes

A large percentage of seismic events observed on the short period components of the Apollo seismic experiment are very small moonquakes, occurring with great regularity. It is believed that many of these events are natural seismic occurrences generated by small shallow moonquakes, about 1.5–4 km distant, triggered by diurnal thermal variations (Duennebier and Sutton, 1974). These events are characterized by (1) signals occurring periodically at times correlating with the lunation period (29.5 days), (2) signals with almost matching waveforms and (3) nearly identical amplitudes. Thermal moonquake activity starts abruptly about 2 days after lunar sunrise and decreases rapidly after sunset (Duennebier and Sutton, 1974).

2.2.4. Meteoroid impacts

Meteoroid impacts are not representative of true lunar seismicity, but do nonetheless provide a unique look of the spatio-temporal pattern of interplanetary objects in the immediate neighborhood of the Earth–Moon system (e.g., Duennebier et al., 1976). The impact of a meteoroid on the surface of the Moon acts as a source generating seismic waves, with only a small fraction of the meteoroids kinetic energy converted to seismic energy (e.g., Melosh, 1989). As shown in Table 2 more than 1700 such events were recorded by the seismic network in its 8 years of operation. The masses of the impacting meteoroids lie in the range from 100 g to 100 kg, with two distinct populations, cometary and asteroidal, identified that cross the Earth–Moon system (Oberst and Nakamura, 1991). Impacts also include those labelled artificial (man-made) impacts and represent impacts of crashing used spacecraft sections onto the lunar surface (third stage of the Saturn launch vehicle prior to landing and the Lunar Module after surface operations and docking with orbiting spacecraft had occurred).

2.3. A summary of recent efforts and the gross lunar structure

For purposes of imaging the very shallow crustal structure (to a few kilometers depth) active seismic experiments, in contrast to the

above passive experiments, were also carried out on missions 14, 16 and 17 (Cooper et al., 1974; Kovach and Watkins, 1973a,b). During Apollo missions 14 and 16 small geophone arrays recorded signals from small explosive sources (thumper charges) that were detonated before the Astronauts had left the Moon, while for the active seismic profiling experiment carried out on the Apollo 17 mission explosive charges were detonated after the astronauts had left the Moon. Recent reanalysis of the dataset acquired from the Apollo 17 geophone array used the passive imaging technique (Larose et al., 2005), which is based on the time-domain cross-correlation of acoustic or seismic waves acquired at two passive sensors (e.g., Sabra et al., 2005; Shapiro and Campillo, 2004). Larose et al. were able to retrieve a well-defined dispersive Rayleigh-wave pulse from which the uppermost crustal structure could be constrained. In addition, the estimated signal-to-noise ratio of the dispersive wave was found to be strongly dependent upon solar illumination, effectively making solar heating a source of seismic noise on the Moon. Further analysis showed that the seismic wave velocity structure beneath the landing site of Apollo 17 varies as a function of temperature on a diurnal basis (Sens-Schönfelder and Larose, 2008; Tanimoto et al., 2008).

Inspite of the problems that have beset lunar seismic data and their interpretation from the beginning, including paucity of stations, their limited spatio-temporal location, restricted instrument sensitivity as well as limited number of usable seismic events (see also Nakamura (2010)), it has nonetheless been possible to extract an arrival-time data set from which inferences on the internal structure of the Moon could be obtained. The resulting dataset which consists of first arriving P- and S-waves only, totaling some 300–400 arrival time readings (compare this with standard terrestrial seismic tomography studies which typically use in excess of 10^4 readings), automatically imparts certain limits on the amount of information that can be extracted. However, the Apollo lunar seismic data constitutes a unique and extremely valuable resource, because it is the only extraterrestrial seismic data set which can be used to infer the interior structure of a planetary body besides the Earth.

Toward the end of the 1970s and early 1980s the last Apollo-era analyses of the entire dataset were undertaken. These revealed the Moon to be a differentiated body, stratified into a crust and mantle of which the lower part is possibly partially molten. These and other features are also observed in more recent independent analyses of the entire Apollo seismic data set (Gagnepain-Beyneix et al., 2006; Khan and Mosegaard, 2002; Khan et al., 2000; Lognonné et al., 2003). Our present-day knowledge of the lunar interior, based on interpretation of the above velocity models, is summarized schematically in Fig. 4. Although a mid-mantle seismic (at 500 km depth) discontinuity figures in the model of Nakamura (1983) it is not necessarily real inasmuch as it was included for computational purposes only. Subsequent models by e.g., Khan and Mosegaard (2002), Lognonné et al. (2003), and Gagnepain-Beyneix et al. (2006) also showed mid-mantle discontinuities at 550 km and ~750 km depth, respectively, whereas the model proposed by Khan et al. (2006a), based on thermodynamic computations (see Section 5.2 for more details) and a chemically uniform mantle, by definition contained no discontinuity in spite of being able to fit data. In short, seismic discontinuities in the mantle then as now remain unresolved (see also discussion in Lognonné and Johnson, 2007).

The presence of a lunar core could not be ascertained due to lack of seismic waves traversing the central part, although a farside impact almost diametrically opposite to station 15 and the peculiar characteristics of signals emanating from the only located farside deep moonquake at the time, gave tentative evidence for a low-velocity core with a permissible radius in the ranges of 170–360 km (Nakamura et al., 1974b) and 400–450 km (Sellers, 1992), respectively, as well as an attenuating, possibly partially molten, region in the lower mantle (Nakamura, 2005; Nakamura et al., 1973; Weber et al., 2010). Recent efforts have been invested in search of elusive core phases and while the results can be construed as indicating a small lunar core (~330–420 km in radius), whose outer part is possibly molten (Garcia et al., 2011; Weber et al., 2010), affirmative evidence is yet to be procured and confirmation of a lunar core will most probably have to await the acquisition of new seismic data.

For completeness, we would like to mention that seismology has not been the only means of probing the lunar interior. Use of magnetic fields and time-of-flight of laser pulses were other means. Briefly, electromagnetic sounding of the Moon (see e.g., Sonnett, 1982 for a detailed review) consists of measurements of the lunar inductive response to time-varying external magnetic fields when the Moon was in the solar wind or terrestrial magnetosheath and have been used to infer the lunar conductivity as a function of depth. Analyses based on magnetometer data from Explorer 35 while in orbit (defining the incident magnetic field) and simultaneous Apollo 12 surface magnetometer data (defining incident as well as induced field) covered the period range of 10^{-3}–10^{-5} Hz enabling sounding of the lunar mantle to ~1200 km

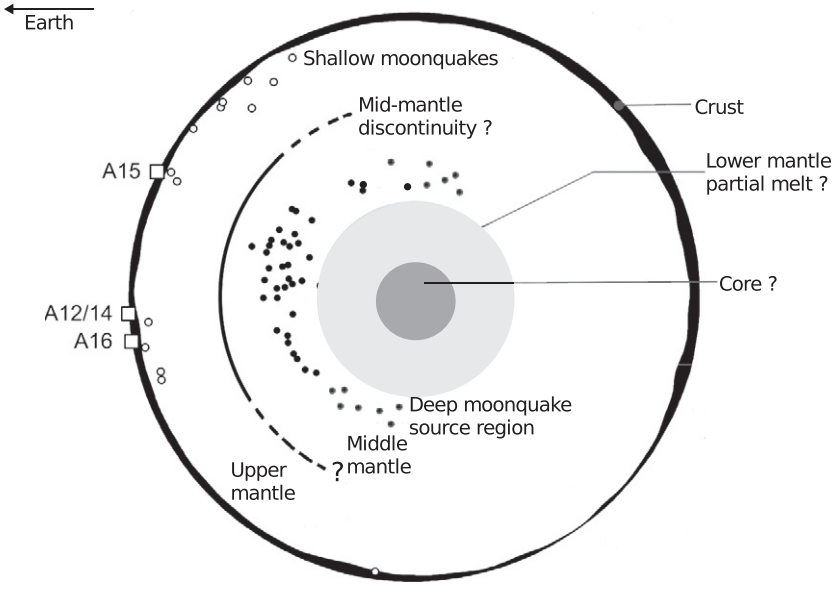

Fig. 4. Schematic diagram of the internal structure of the Moon as seen from the point of view of lunar seismology. Structure deeper than the location of deep moonquakes is subject to large uncertainty. A12–A16 indicate relative location of Apollo lunar seismic stations. Modified from Wieczorek et al. (2006).

depth (e.g., Hobbs, 1977; Hood et al., 1982a; Khan et al., 2006b; Wiskerchen and Sonett, 1977). Electrical conductivity was found to rise from 10^{-4}–10^{-3} S/m at a few hundred kilometer depth to roughly 10^{-2}–10^{-1} S/m at about 1100 km depth in agreement with laboratory electrical conductivity measurements of olivine and orthopyroxene at lunar conditions. Additional efforts have focused on converting these conductivity bounds, through the use of laboratory measurements of mineral electrical conductivity, to constraints on the lunar temperature profile (e.g., Hood & Sonett, 1982; Hood et al., 1982b; Huebner et al., 1979) as well as mantle composition (e.g., Khan et al., 2006b). Future efforts hold the potential of considerably improving these results (e.g., Grimm and Delory, 2012).

The lunar laser ranging (LLR) experiment, the only still-ongoing surface experiment deployed during the Apollo missions, consists of high-accuracy measurements of the distance between a set of retro-reflectors placed on the lunar surface (Apollo missions 11, 14 and 15, as well as both Soviet Lunokhod reflectors with the recent rediscovery of Lunokhod-1) and a number of observatories on Earth, through the round-trip travel time of the laser pulse. Any changes in the distance manifest itself as a change in travel time (for a review of LLR see Dickey et al. (1994)). Analysis of LLR data has improved knowledge on the dynamics and the structure of the Moon, through very accurate determination of the second- and third-degree gravitational harmonics, the moments of inertia and their differences as well as the lunar tidal Love number which all depend on the lunar internal mass distribution, composition and dynamics. From analysis of more than 30 years of LLR data Williams et al. (2001) detected a displacement of the Moon's pole of rotation indicating that dissipation is acting on the rotation, which arises from 1) monthly solid-body tides raised by the Earth and Sun, and 2) a fluid core, with a rotation distinct from that of the solid body. Independent analyses of LLR-derived data confirms the latter (e.g., Khan and Mosegaard, 2005; Khan et al., 2004).

3. Seismic velocity structure—a closer look

Completion of processing of all the lunar seismic data collected during the 8 years of the Apollo seismic network operation in the late 1970s and early 1980s resulted in a set of arrival times from which the lunar velocity structure could be inferred (Nakamura, 1983). Prior to this several groups had been able to determine major features of the lunar interior using more limited data sets then available (e.g., Goins et al., 1981b; Nakamura et al., 1974b; Toksöz et al., 1974). Recent reanalysis of the entire data set by Lognonné et al. (2003) and Gagnepain-Beyneix et al. (2006) has resulted in an independent data set, in addition to expansion of the original Nakamura (1983) data set by Nakamura (2005) through inclusion of an enlarged deep moonquake catalog (this expanded set of deep moonquake arrival-time picks is yet to be analyzed).

These recent independent efforts are important inasmuch as the lunar seismic data set is limited, which, given the complex character of the signals, renders, in principle, the simple process of reading first-arrivals highly complicated and therefore prone to subjectivity (see e.g., appendix A of Nakamura (2005) for differences in actual arrival-time picks among different investigators). If, however, the data set is large enough these inconsistencies will be smoothed out and the final results of the inversion are less likely to be biased. On the other hand, if the data set is not characterized by this redundancy, as is the case here, objectivity cannot be attained and differences in data interpretation among different observers can significantly alter the models obtained. It is indeed the case that, whichever inverse method is used, the results obtained by different scientists from such data sets are different (e.g., Tarantola, 2005).

The Apollo lunar seismic data set illustrates this situation excellently. During the Apollo era two data sets were under consideration, one by the MIT group (e.g., Goins et al., 1981b) and the other one by the Galveston group (University of Texas) (e.g., Nakamura et al., 1982). While differing not only in individual arrival time readings, they also differed in number, notably of deep moonquakes. Despite the fact that both groups employed linearized techniques to invert data, different inversion results and hence interpretations of the lunar internal structure were obtained.

This state of affairs has not improved considerably with more recent attempts. In an effort to re-evaluate the entire lunar seismic data J. Gagnepain-Beyneix (IGP Paris) has independently constructed a third set of arrival-time readings, which has been employed in a series of recent studies that, like the Apollo-era lunar seismic models, tend also to be accentuated by differences (e.g., Chenet et al., 2006; Gagnepain-Beyneix et al., 2006; Garcia et al., 2011; Khan et al., 2007; Lognonné et al., 2003). In this context, and in view of the actual arrival-pick differences among different investigators (Nakamura, 2005), attempts by Garcia et al. (2011, 2012) at constructing the equivalent of a preliminary lunar reference model must be considered premature.

The final Apollo-era velocity model of Nakamura (1983, NK83) and the recent models of Khan et al. (2000) and Gagnepain-Beyneix et al. (2006) are shown in Fig. 5. These latter models have been obtained using modern-day inversion and analysis techniques. The models of Khan et al. (KH00) and Khan and Mosegaard (2002, KM02) rely on a Monte Carlo-based sampling algorithm (Markov chain Monte Carlo method) to invert the same data set considered by Nakamura (1983), with the purpose of providing more accurate error and resolution analysis of inverted velocity models than is possible with linearized techniques. The models of Lognonné et al. (LG03) and Gagnepain-Beyneix et al. (2006) (GPB06) are derived on the basis of a purely random search of the model space to invert their independently read data set, which consists of 8 (7) artificial impacts, 19 (18) meteoroid impacts, 8 (14) shallow moonquakes, and 24 (41) deep moonquakes with parentheses indicating the number of sources considered by Nakamura. LG03 and GPB06 also employ the receiver function (S-to-P conversion) data of Vinnik et al. (2001) to additionally constrain location of velocity discontinuities in the crust beneath station 12.

For completeness, we should note that in addition to the standard one-dimensional travel time inversions mentioned above Zhao et al. (2008), has, presented a three-dimensional seismic tomography model of the Moon, which, given the large uncertainties involved, must be considered as very preliminary, while Garcia et al. (2011) have inverted the travel time data of LG03 using the simplified Adams-Williamson equation of state. The latter assumes adiabatic compression of an isochemical material devoid of any mineral phase changes, coupled with a Birch-type linear relationship between seismic velocity and density. However, since effects of temperature play a more significant role in determining variations of physical properties with depth in the Moon than pressure, neglect of the former contribution results in physical properties, in particular S-wave velocities, that increase with depth rather than decrease or remain constant as expected for present-day lunar temperature gradients (see also discussion in Section 5.2 and Fig. 11).

The inversion problem for the crustal seismic velocity model was simplified through application of astronaut-activated seismic energy sources and nearby impacts of the Lunar Module (LM) ascent stage and third stage of the Saturn launch vehicle (S-IVB) whose event times, energies, and positions were accurately known. In comparison, origin times and positions of the naturally occurring sources had to be determined prior to or, at least, concomitantly with the structural parameters. Consideration of source–receiver geometry to some extent also plays a role, since rays from other sources than the man-made impacts tend to traverse the crust beneath each recording station in an almost vertical sense with ensuing limited sensitivity to structure. These events (7 in total) cover epicentral distances between 9 and 1750 km. However, because of the sequential emplacement of the stations and the limited amount of energy available not all impacts were recorded (Table 3). Moreover, because of the particular signal characteristics of impacts (see Fig. 3), only P-wave arrivals could be extracted, while S-waves are very difficult to extract from the coda.

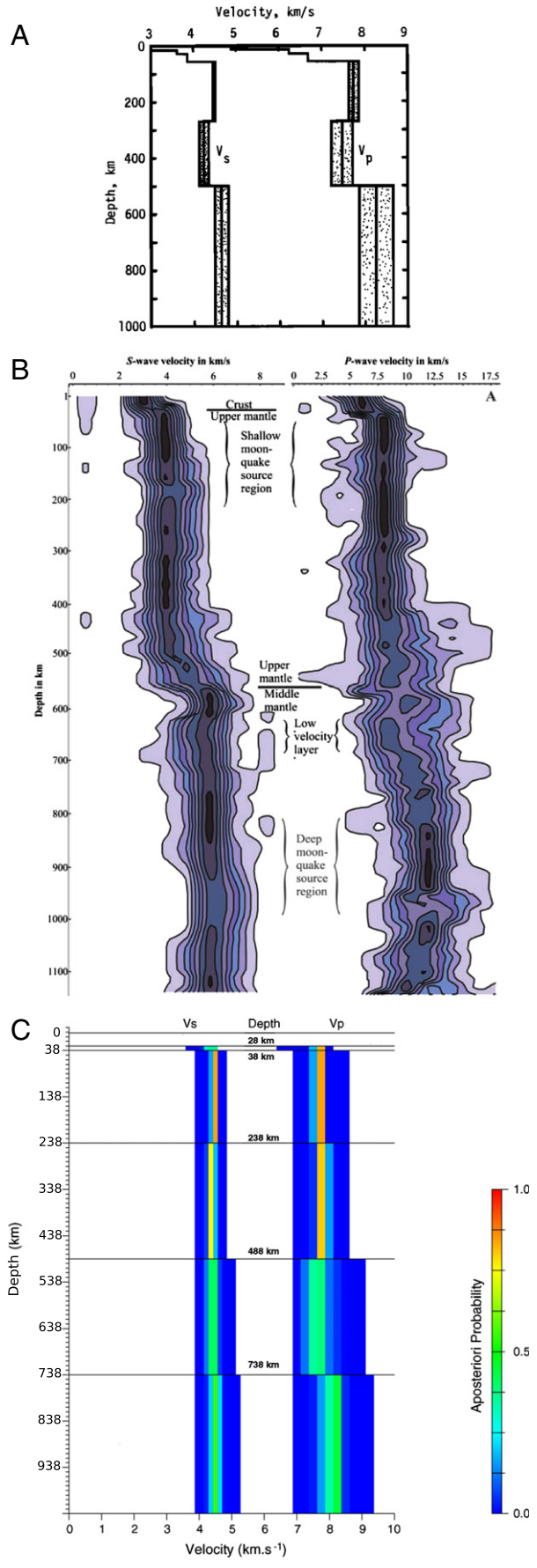

Of immediate importance for structural inversions are differences in arrival-time picks (here summarized as travel-time picks), which are easily seen to reach 3–4 s. Upper and lower mantle structure were constrained by inversion of shallow moonquakes, meteoroid impacts, and deep moonquakes, respectively.

3.1. Structural features of the lunar crust

Toksöz et al. (1974) calculated a crustal P-wave velocity model (TK74) valid for the Mare Cognitum region near the Apollo 12 and 14 landing sites, and within the Procellarum KREEP Terrane (Jolliff et al., 2000), using the results obtained from the active lunar seismic profiling experiment (LSPE) of Kovach and Watkins (1973a, 1973b) to constrain the very near-surface velocity structure (0–2 km depth). This model is shown in Fig. 6 together with the recently proposed models of Khan et al. (2000) and Lognonné et al. (2003).

A continuous layer known as "regolith" covers the entire lunar surface. This superficial layer consists of very low-velocity material with P-wave velocity (V_P) of around 100 m/s and ranging in thickness between 3.7 and 12.2 m at the Apollo landing sites (Nakamura et al., 1975). Constituents range from very fine dust to blocks and boulders several meters across. Experiments have revealed a similarity in seismic characteristics at all sites (maria and highlands) with values ranging over the different Apollo sites from 99 to 114 m/s (Cooper et al., 1974). This is thought to indicate that the processes producing the regolith formed material of uniform seismic properties Moon-wide from different mare and highland source materials (Nakamura et al., 1975). The top layer is very loose, while lower depths become strongly compacted.

In all seismic models velocity increases rapidly in the upper few kilometers due to rocks with different microcrack properties (Simmons et al., 1975). It is believed that the continuous increase in compressional velocity between the upper first kilometer and 20 km depth is primarily ascribable to the effect of crack closure with increasing pressure. The cracks are considered to have been either induced by the shock effects of impacts and/or as a result of thermal history and cooling processes. In the absence of fluids such cracks would not anneal at low pressures and temperatures. Thus, the continuous increase in velocity from the upper to mid-crust is because of the transition from regolith over fractured rocks to competent crustal materials as pressure increases. The mid-crustal discontinuity in the depth range of 10–20 km depth (20 km—TK74,~15 km—KH00, and ~10 km depth—LG03), which is prominent in all studies, was initially identified as the base of mare basalts (Toksöz et al., 1972), given tentative evidence for a similar discontinuity beneath the Apollo 16 highland site (Goins et al., 1981c). Presently, the notion of a compositional change is favored (Todd et al., 1973; Toksöz et al., 1974), given that data from material within the floor of the South-Pole Aitken basin and central peaks of some impact craters strongly suggest a crust that varies both laterally and vertically in composition (e.g., Cahill et al., 2009; Lucey et al., 1995; Tompkins and Pieters, 1999; Wieczorek and Zuber, 2001; Wieczorek et al., 2006).

3.2. Lunar Moho and upper mantle

All three seismic velocity models (TK74, KH00 and LG03) shown in Fig. 6 appear to be almost constant between 20 km and the base

Fig. 5. Seismic P- and S-wave velocity models of the lunar crust and mantle. A) Apollo-era model of Nakamura (1983). Used by permission of the American Geophysical Union, from Nakamura et al. (1983), Journal of Geophysical Research, Vol. 88, Fig. 2, p. 683. B) Model derived from non-linear inversion of Khan et al. (2000). The marginal probability of the seismic velocity is plotted at one-kilometer depth intervals, and the contours define nine equally-sized probability intervals. Used by permission of the American Geophysical Union, from Khan et al. (2000), Geophysical Research Letters, Vol. 27, Fig. 1a, p. 1592. C) Model obtained from the inversion of Gagnepain-Beyneix et al. (2006). Colour bar indicates probability (normalized). Reproduced from Gagnepain-Beyneix et al. (2006), Physics of the Earth and Planetary Interiors, 159, Fig. 8, p. 151 with permission from Elsevier.

Table 3
Summary of artificial impact P-wave travel time readings. NK83, LG03, and GPB06 refer to Nakamura (1983), Lognonné et al. (2003), and Gagnepain-Beyneix et al. (2006), respectively. LM refers to Lunar Module and S-IVB to the upper stage of the Saturn V rocket. For the Apollo 16S-IVB impact (entries marked *a*) tracking signal was lost before the module impacted the Moon, leaving impact location and time unknown. For this reason impact of S-IVB 16 is not considered part of the artificial impacts in Nakamura (1983). Lognonné et al. (2003) have likely used the estimated impact coordinates and time from the Apollo 16 Preliminary Science Report, NASA SP-315, that were based on the seismic data and thus very uncertain (uncertainties in latitude, longitude and impact time are: ±0.7° N-S, ±0.2° E–W, ±4 s). Note that in the study of GPB06 this particular event was discarded.

Object	Station	Distance (km)	Travel time (s) NK83	Travel time (s) LG03/GPB06
LM 12	12	73	–	24.7
S-IVB 13	12	135	28.6	27.8
S-IVB 14	12	172	35.7	35.4
LM 14	12	114	25	21.1
	14	67	17.8	18.8
S-IVB 15	12	355	55	54.1
	14	184	36.6	36.8
LM 15	15	93	22	27.5
S-IVB 16	12	*a*	–	27.4
	14	*a*	–	43.5
	15	*a*	–	146.9
S-IVB 17	12	338	56	55.7
	14	157	32	32.2
	15	1032	151	154.2
	16	850	123.1	121.9
LM 17	17	9	5.8	–

of the crust, the “lunar Moho”, consistent with a compositionally homogeneous lower crust. Assuming the definition of Steinhart (1967) for the Moho as the depth where the P-wave velocity is first observed to increase discontinuously or steeply to a value between 7.6 km/s and 8.6 km/s, the seismically inferred lunar crustal thickness appears model dependent with values (see Table 4) ranging from the Apollo-era canonical value of 60 km (TK74) to the more recent estimates of ~38–45 km (KH00, KM02) and 30 km (LG03), respectively, although lower crustal thickness estimates of 50–55 km had also been proposed in the Apollo-era (Latham et al., 1973).

Differences in crustal thickness estimates between Apollo-era and recent models are discussed in detail in Khan and Mosegaard (2002). Briefly, model TK74 additionally considered amplitude data, secondary arrivals, and synthetic seismograms as a means to constrain their crustal model further. However, independent reassessment of these data showed that amplitudes could be fit equally well with a shallower crust-mantle interface, while uncertainties on secondary arrivals and synthetic seismograms are too large to render these usable. Discrepancies in crustal thickness between the recent models KH00 and LG03 are related to a combination of factors, including disparate travel-time readings (data), inversion technique (methodology), and model parameterization. As an additional observation, it might be remarked that in model LG03 impact S-IVB 16 is employed as an artificial impact, i.e., assuming location and impact time known. However, tracking signal was lost for S-IVB 16 before it impacted on the Moon, leaving impact location and time unknown. Given the large uncertainties involved (uncertainties in longitude, latitude and impact time are, respectively, ±0.7° N–S, ±0.2° E–W, and ±4 s) (Apollo 16 Preliminary Science Report, NASA SP-315) and the small number of artificial impact events available that ultimately constrain crustal structure (see also the discussion in Section 3), a bias is very likely to result by the presence of such potential “outliers". The point here is to emphasize the importance of subjectivity when working with small data sets where differences in and number of readings can easily translate into differences in final model.

Differences in crustal thickness between models KH00 and KM02 result from differences in *a posteriori* analysis of the crustal models. Specifically, in KM02 Bayesian hypothesis testing was employed to search among the models obtained in KH00 for those that satisfied the criteria of having either relatively shallow lunar Mohos (ranging from 35 to 45 km depth) or relatively deep lunar Mohos (ranging from 50 to 70 km depth). In this manner crustal thickness was narrowed further relative to the value obtained in KH00.

It has also recently been discovered (Nakamura, 2011) that the near-surface structure derived from the Apollo 17 seismic profiling experiment (e.g., Cooper et al., 1974) is erroneous because of a problem related to how timing information was stored when data were radioed back to Earth. This may have implications for the validity of models of the internal velocity structure that rely on this very shallow-structure model. In particular, earlier estimates of crustal structure were influenced by artificial impact LM 17 as observed at Apollo station 17, which is now found to be in error, and thus produced a thicker crust than the true thickness (pers. comm., Y. Nakamura, 2013).

As discussed by Wieczorek et al. (2006) estimates of the average crustal thickness based on inversions of gravity and topography data (see next section) are more consistent with these recent thin-crust estimates than the Apollo-era value of 60 km. Ishihara et al. (2009), using the SELENE gravity and topography models, presented a lunar crustal thickness model whose crustal thicknesses beneath Apollo 12 and 14 landing sites were found to be 45.1 and 49.9 km, respectively, consistent with the crustal thickness estimate of model KH00, but only marginally so with the estimate of KM02. Ishihara et al. also found that if they employed the crustal thickness estimate of LG03 or Chenet et al. (2006), who searched for lateral variations in lunar crustal thickness, negative crustal thickness values, corresponding to exposed mantle materials, would be obtained within several basins. This, they argued, is highly unlikely, as any such negative crustal thickness areas would occupy not only mare basalt covered areas, but also highland crust exposed areas. However, analysis of high-resolution gravity and topography data recently acquired by the GRAIL Discovery mission (see Section 4) has obtained new information regarding crustal density that eliminates the inconsistency of global crustal thickness models with these results.

In spite of modeling and data discrepancies among the various investigations summarized here, a reasonable conclusion, based on the recent seismic studies, appears to be that in the immediate vicinity of Apollo stations 12 and 14 the lunar Moho is shallower than previously thought, with estimates lying in the range of 30–45 km.

By analogy with the Earth, the zone below the base of the crust is referred to as the mantle. All three models shown in Fig. 5 depict, within uncertainties of the models, constant velocities to depths of >200 km suggesting a largely homogeneous upper mantle. Regarding absolute P- and S-wave mantle velocities the models are generally consistent (see Table 5). Differences in estimated seismic velocities and uncertainties are primarily linked to data and inversion method employed. The velocities determined for the upper mantle of the Moon are very close to the average for rocks of the upper mantle of the Earth. The seismic attenuation structure (Q_P and Q_S) of the lunar crust and upper mantle likely resides in the range of 4000–7000 on account of the characteristics of HFTs, implying temperatures well below the solidus and absence of volatiles (Nakamura and Koyama, 1982; Nakamura et al., 1974a).

4. Studies of the lunar Moho using gravity and topography

4.1. Bouguer gravity anomaly and crustal thickness

The Apollo spacecraft, in near-equatorial orbits, provided the earliest glimpses of the crustal structure of lunar basins and revealed a hemispheric asymmetry in crustal thickness (Kaula et al., 1972). More extensive analysis of the lunar crust became possible with the 1994 Clementine Mission (Nozette et al., 1994), which carried a laser altimeter (Smith et al., 1997). Tracking of an orbiting spacecraft such as Clementine senses variations in gravitational attraction of the

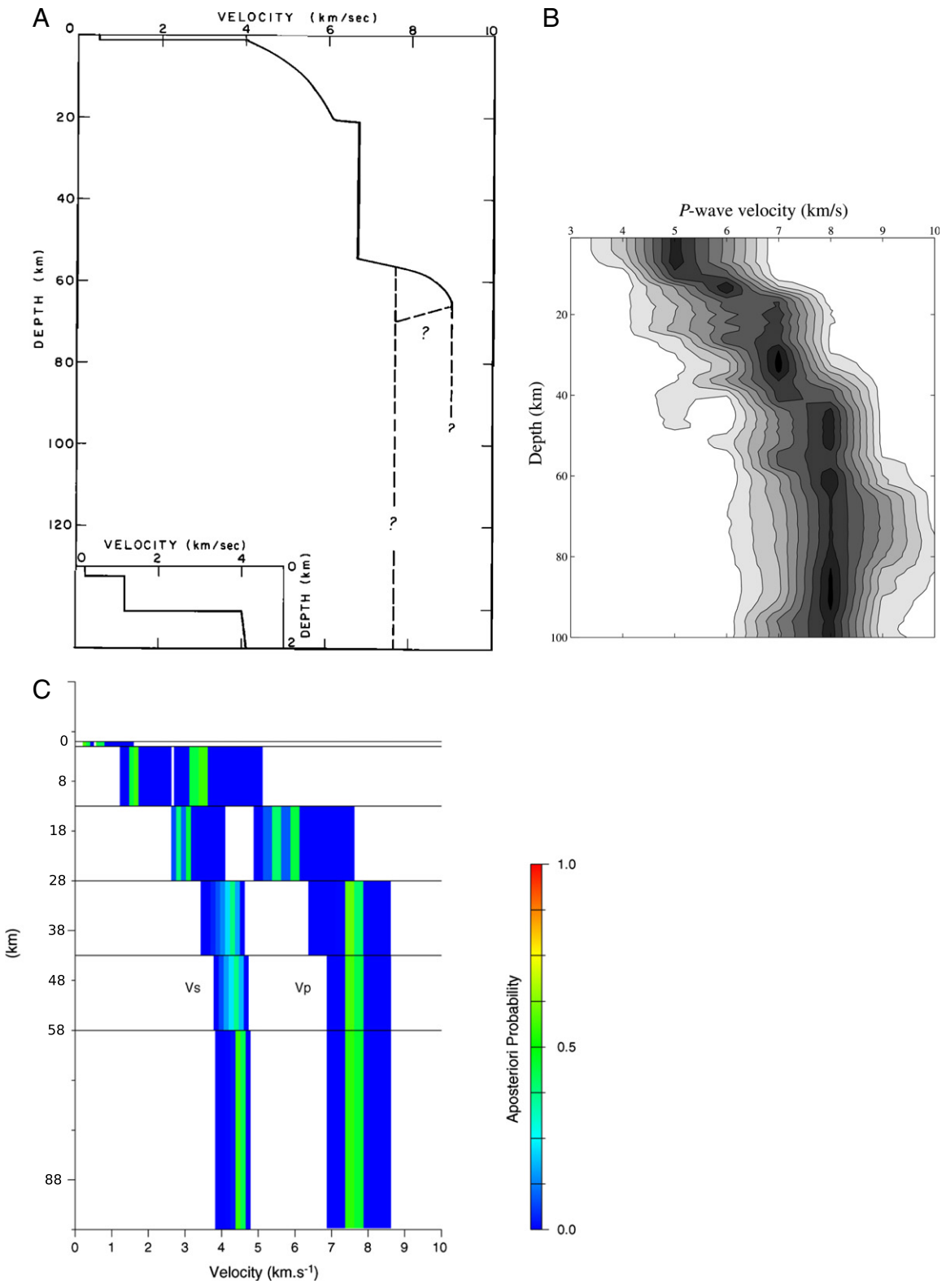

Fig. 6. Crust and upper mantle models of the lunar P-wave velocity structure to ~100 km depth. Left: Apollo-era P-wave velocity model from Toksöz et al. (1974). Inset shows the near-surface structure used (from the study of Kovach and Watkins (1973a,b)). "?" indicates uncertainty in upper mantle velocity structure. Used by permission of the American Geophysical Union, from Toksöz et al. (1974), Reviews of Geophysics, 12, Fig. 19, p. 539. Center: P-wave velocity model derived from the non-linear inversion of Khan et al. (2000). The marginal probability of the seismic velocity is plotted at one-kilometer depth intervals, and the contours define nine equally sized probability intervals. Used by permission of the American Geophysical Union, from Khan et al. (2000), Geophysical Research Letters, Vol. 27, Fig. 1b, p. 1592. Right: P-wave velocity model obtained from the inversion of Lognonné et al. (2003). Colour bar indicates probability (normalized), while the black line represents the most likely model. Reproduced from Lognonné et al. (2003), Earth and Planetary Science Letters, 211, Fig. 3, p. 33 with permission from Elsevier.

Table 4
Summary of seismically-determined crustal thickness estimates.

Study	Crustal thickness (km)
Toksöz et al. (1974)	60 ± 5
Nakamura (1983)	58 ± 8
Khan et al. (2000)	45 ± 5
Khan and Mosegaard (2002)	38 ± 3
Lognonné et al. (2003)	30 ± 2.5

body relative to that of a central mass, while measuring topography in the same coordinate frame, providing powerful constraints on internal structure. Much of the observed gravity anomaly arises from the contrast in density between surface rocks and space in the vicinity of mountains and craters, which can be modeled using topography and rock densities. The gravity signature of the topography is then subtracted from the observed gravity to yield a Bouguer potential anomaly. Inversion of the Bouguer anomaly by downward continuation to the crust–mantle density interface yields global models of the variations in crustal thickness about some mean value (e.g., Zuber et al., 1994).

Gravity inversions place minimum and maximum constraints on the thickness of the crust. The average thickness must be sufficient to avoid negative thicknesses over positive anomalies. Conversely, the attraction of mantle topography is filtered by upward continuation to the surface, so greater topographic variation is required to produce the same Bouguer anomaly at a greater depth. The need to fit gravity with physically plausible amplitudes therefore places a maximum constraint on average crustal thickness.

Crustal models can be tied to anchoring points where seismic estimates of crustal thickness have been made (e.g. Hikida and Wieczorek, 2007; Khan et al., 2000; Lognonné et al., 2003; Nakamura et al., 1979; Toksöz et al., 1974). Neumann et al. (1996) presented crustal thickness models based on the gravity model GLGM-2 (Lemoine et al., 1997) tied to a 55-km thickness beneath Apollo stations 12 and 14 resulting in a global mean thickness of 61 km. A minimum crustal thickness of 20 km was found at the Orientale, Crisium and Humorum mare basins suggesting that a thinner crust would have been feasible. Models exploring single and dual crustal layers (Wieczorek and Phillips, 2000) led to a 60 km constraint on mean thickness, but the model resolution was limited by the quality of the gravity data to spherical harmonic degree 30, equivalent to a spatial block size of 182 km, leaving much of the crustal structure of basins unresolved. Moreover the laser altimetry from Clementine was particularly sparse over the rough highland terrain, and suffered in places from ranging errors of many kilometers (e.g., Margot et al., 1999).

The Lunar Prospector (LP) spacecraft launched in 1998 provided greatly improved gravity (Konopliv et al., 1998) from low-altitude two-way Doppler tracking over the nearside. Perturbations of the spacecraft orbit as it emerged from occultation revealed several new farside basins with positive gravity anomalies (mascons) over topographic depressions, in addition to those of the five large nearside mare basins. LP also detected mascons over minimally filled basins or basins without mare, suggesting that much of the positive anomaly arose from dense uplifted mantle plugs, the result of mantle rebound following impact, rather than subsequent surface loading. The Clementine and LP studies could only infer farside gravity anomalies from perturbations of the spacecraft orbit after exiting from lunar occultation, as there was no direct radio tracking over the farside. A Clementine photogrammetric solution ULCN2005 (Archinal et al., 2006) improved topographic knowledge over the north and south poles where the lidar could not reach, but km-scale errors in topography over the farside remained. Wieczorek et al. (2006) used the gravity solution LP150Q (Konopliv et al., 2001) to explore the constraints on crustal thickness, generating models with uniform and/or stratified crust with an average thickness of 49 km. Subsequent inversions with ULCN2005 topography (Hikida and Wieczorek, 2007) found a 43 km lower limit on average thickness.

Table 5
Summary of P- and S-wave mantle velocities in selected lunar models.

Study	P-wave velocity (km/s)	S-wave velocity (km/s)
Nakamura (1983)	7.74 ± 0.12	4.49 ± 0.03
Khan et al. (2000)	8.0 ± 0.8	4.0 ± 0.4
Lognonné et al. (2003)	7.63 ± 0.05	4.5 ± 0.07

4.2. Recent improvements in topography and gravity

The SELENE (Kaguya) mission, with a full complement of remote sensing instruments, was launched in September 1997, followed by launches of the Chang'E-1 (October 1997), Chandrayaan-1 (October 2008) and Lunar Reconnaissance Orbiter (LRO) (June 2009) missions. The Kaguya lunar explorer carried the LALT laser altimeter (Araki et al., 2009) which ranged at 1 Hz from a 100-km-altitude polar orbit, eventually returning 22 million global topographic measurements before the spacecraft impacted the surface in 2009. Typically 40-m-diameter laser footprint ranges with 5 m vertical accuracy were collected at 1.6 km intervals along-track (Araki et al., 2009). Precision geolocation of over 10 million ranges resulted in a degree and order 359 (STM359_grid-03) spherical harmonic topographic model. The LAM instrument on Chang'E-1 provided the CLTM-s01 model (Ping et al., 2003) with somewhat fewer measurements, while the LLRI instrument on Chandrayaan did not achieve global coverage.

The primary and extended missions of the Lunar Reconnaissance Orbiter (LRO) as of the end of 2012 have returned over 6 billion measurements from the Lunar Orbiter Laser Altimeter (LOLA) instrument (Smith et al., 2010), achieving better than 1 m radial and 30 m total position accuracy on ~5-m-diameter footprints. Firing at 28 Hz with five laser spots, LOLA has produced terrain models at resolutions as fine as 60 m (Fig. 7) with 10-m resolution near the poles (Zuber et al., 2012). The few near-equatorial gaps in coverage wider than 1 km, due to the LRO polar orbit ground track spacing, are inconsequential for geophysics. LOLA's highest elevation occurs north of Korolev basin at 5.4°N, 201.4°E, reaching 10.79 km above a 1737.4 km spherical datum. The 2400-km-diameter South Pole-Aitken (SP-A) basin to the south contains the lowest point, −9.12 km, within Antoniadi Crater. The range of elevation is 25% greater than that of the ~72,500 measurements obtained by the Clementine lidar (Smith et al., 1997). Continued mapping and analysis of stereoscopic imaging by Kaguya's Terrain Mapping Camera (Haruyama et al., 2009) and the Lunar Reconnaissance Orbiter Camera (Scholten et al., 2012) in conjunction with laser altimetry will provide further improvements in resolution and coverage.

The quality and resolution of lunar gravity has likewise improved dramatically in the last six years. The SELENE mission incorporated limited four-way Doppler tracking using a high-altitude relay satellite visible from Earth (Namiki et al., 2009). The Kaguya explorer was the first spacecraft tracked directly over the farside and it provided gravity models complete to degree and order 100 (Matsumoto et al., 2010), and later 150 (Goossens et al., 2011) when combined with historical tracking. The remote relay tracking resulted in a reduction in gravity anomaly formal errors from ~100 mGal to under 30 mGal on the farside ($1\ \text{mGal} = 10^{-5}\ \text{m/s}^2$). Mascon-like gravity anomalies were resolved over several farside impact basins. Such anomalies result in large positive Bouguer anomalies that indicate large excursions in crustal thickness and correspondingly shallower and deeper underlying mantle over the Apollo, Moscoviense and Poincaré farside basins as well as nearside basins Crisium and Orientale.

Using updated gravity and topography data, Ishihara et al. (2009) analyzed crustal thickness following the methodology of Wieczorek and Phillips (1998), finding the thinnest crust within the Moscoviense impact basin, with a mean crustal thickness of 53 km, in contrast to previous models that placed the thinnest crust within nearside basins. This study

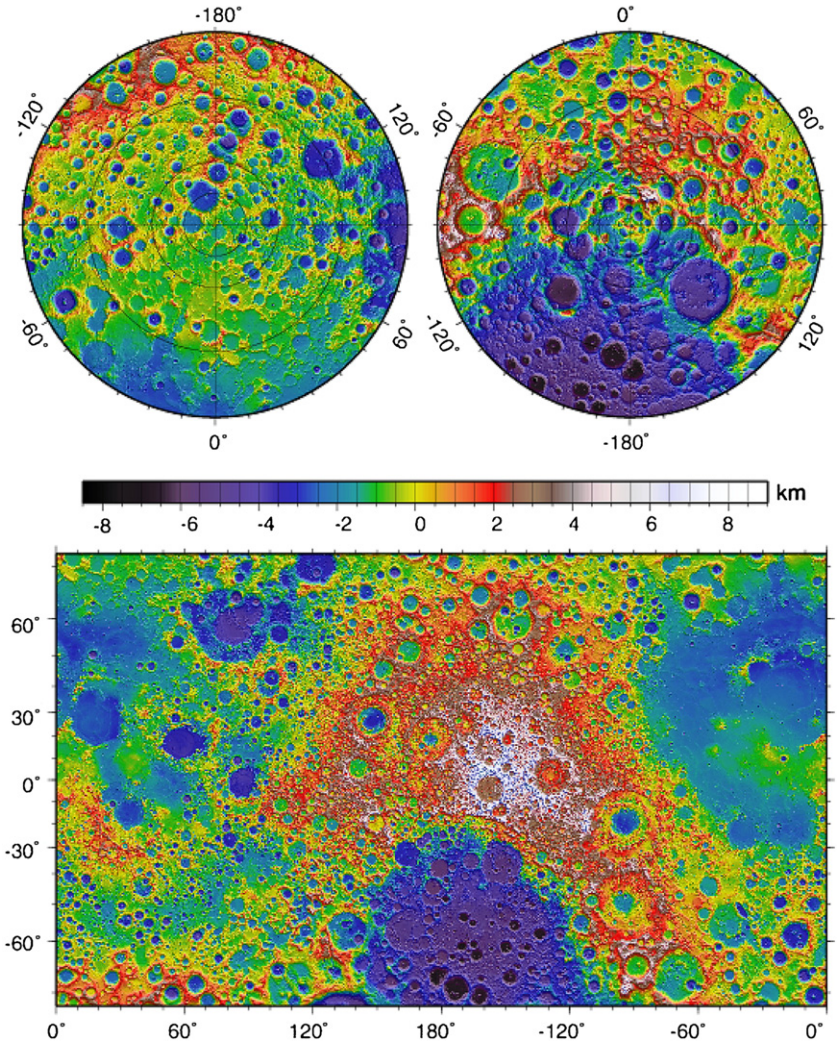

Fig. 7. LOLA Topography relative to a sphere of radius 1737.4 km, over shaded relief. Images are in Mercator projection to 72° N/S, and in polar stereographic projection from 60° to 90° from north and south poles, preserving circular features.

determined the thickness of the crust at the Apollo 12/14 sites to be at least 45–50 km, about 10 km thinner than assumed by Neumann et al. (1996), but inconsistent with the seismic crustal thickness estimates of Lognonné et al. (2003) and Chenet et al. (2006) as discussed previously (see Section 3.2).

With the improved gravity solutions the SELENE investigators were able to distinguish between farside impacts in thicker crust that resulted in smaller amounts of crustal thinning (type I), and impacts in thinner crust that resulted in greater mantle uplift (type II), as well as the mare mascon basins found in previous experiments.

The GRAIL mission (Zuber et al., 2013a), launched September 10, 2011, consisted of two co-orbiting spacecraft that obtained continuous high-resolution gravity measurements by intersatellite ranging. Developed for the sole purpose of measuring gravity and interior structure, the mission conducted its primary measurement phase at a 55-km mean altitude from March to June 2012 and achieved 100% coverage. The GRAIL Ka-band radar observations have produced a spherical harmonic potential model to degree and order 420 that resolves wavelengths as fine as 26 km (Zuber et al., 2013b). Lunar Gravity Ranging System (LGRS) velocity residuals from this model, typically 0.02 ± 0.05 μm/s, are orders of magnitude better than achievable by Earth-based Doppler tracking of spacecraft. Higher-resolution fields will ultimately be derived from the three-month GRAIL extended mission at a 23-km mean altitude that ended with impact on December 17, 2012.

The GRAIL spherical harmonic potential model GL0420A (expanded to degree and order 384) of lunar gravity anomalies is shown in Fig. 8. Major mare basins are visible as large positive mascons, while the fine structure closely resembles the topography. The gravity anomaly represents the integrated attraction of density variations throughout the interior, but the most readily visible short-wavelength features arise from the topography of circular impact structures. Mare basins (Imbrium, Serenitatis, etc.) manifest gravity highs over topographic lows, but typically craters smaller than 300 km in diameter without mare fill give rise to negative anomalies. Such craters correspond to spherical harmonic degrees higher than 60. Beyond degree 150, flexural compensation of topography by deflection of the crust-mantle boundary makes little contribution to the observed gravity field, and the gravity signal is highly correlated with that predicted by surface relief of a uniform-density crust. In such a case a linear transfer function approach (restricted to short wavelengths) provides estimates of the bulk crustal density at depth scales commensurate with topographic variation. The GRAIL data imply a mean bulk density of 2550 kg/m^3 over the farside highlands, considerably lower than the 2800 to 2900 kg/m^3 previously assumed in geophysical studies. The lower density is attributed to impact-induced fractures, implying an average porosity of 12%. The substantial reduction in density due to porosity allows models with crustal thickness more consistent with the recent seismic estimates.

Fig. 9 shows a crustal thickness map of the Moon derived from GRAIL gravity data (Wieczorek et al., 2013) provided as Model 1 online (http://www.ipgp.fr/wieczor/GRAILCrustalThicknessArchive/).

Upper mantle density was assumed to be 3220 kg/m^3. Regional estimates of crustal grain density were derived from remote sensing xestimates of composition. Crustal bulk density was assumed to vary with grain density, reduced by a constant porosity of 12%. The average crustal thickness of 34 km was chosen to fit a thickness of 30 km at the Apollo 12 and 14 sites and attains a minimum thickness of 0.5–1.5 km within the Crisium and Moscoviense basins, while a maximum thickness of 67 km is attained northeast of Korolev basin. The thickest crust on the Moon is located in the farside highlands over the southern rim of the Dirichlet-Jackson basin near 200°E, 7°N (Ishihara et al., 2009; Neumann et al., 1996; Zuber et al., 1994). This location corresponds to the highest lunar topography and lies just outside the rim of the giant South Pole-Aitken basin, where impact ejecta likely added to the already thicker lunar highlands. Exploring tradeoffs between the average crustal thickness and mantle density within plausible ranges, Wieczorek et al. (2013) find a maximum thickness of 80 km in this location.

4.3. Crustal density assumptions

The velocity interface between the mainly anorthositic crust and a more mafic mantle, the seismologically-determined Moho, also represents an increase in density. The density contrast between crust and mantle controls, to first order, the limits that can be placed on the average crustal thickness, as variations in Bouguer gravity due to relief on the Moho are proportional to such contrast. The GRAIL data now allow further exploration of the densities assumed for lunar structure. The density of the upper mantle lies within a range of 3220–3420 kg/m^3, while the bulk density of crustal rocks varies widely with composition and porosity, from approximately 2300 to 2900 kg/m^3 (Wieczorek et al., 2013). In the lunar highlands, where the majority of the crust is located, the bulk density of the crust was estimated at 2550 ± 18 kg/m^3, Huang and Wieczorek (2012), using localized spectral admittance analyses and pre-GRAIL gravity and topography, found an average density of 2691 ± 71 kg/m^3 for the far-side highlands. This study calculated the porosity of the upper few kilometers of crust to be at least 5–10% or more. Han et al. (2011) analyzed low-altitude Lunar Prospector nearside gravity, and while not explicitly solving for density, also obtained admittances that implied substantial porosity over the nearside. These densities result in effectively greater Moho density contrast than typically adopted for geophysical models prior to GRAIL.

The major element composition of the crust, particularly Fe and Ti, can be estimated from multispectral remote sensing (e.g., Lucey et al., 1995) and gamma-ray spectroscopy (Prettyman et al., 2002). The major elements closely predict the grain density of lunar samples via an empirical

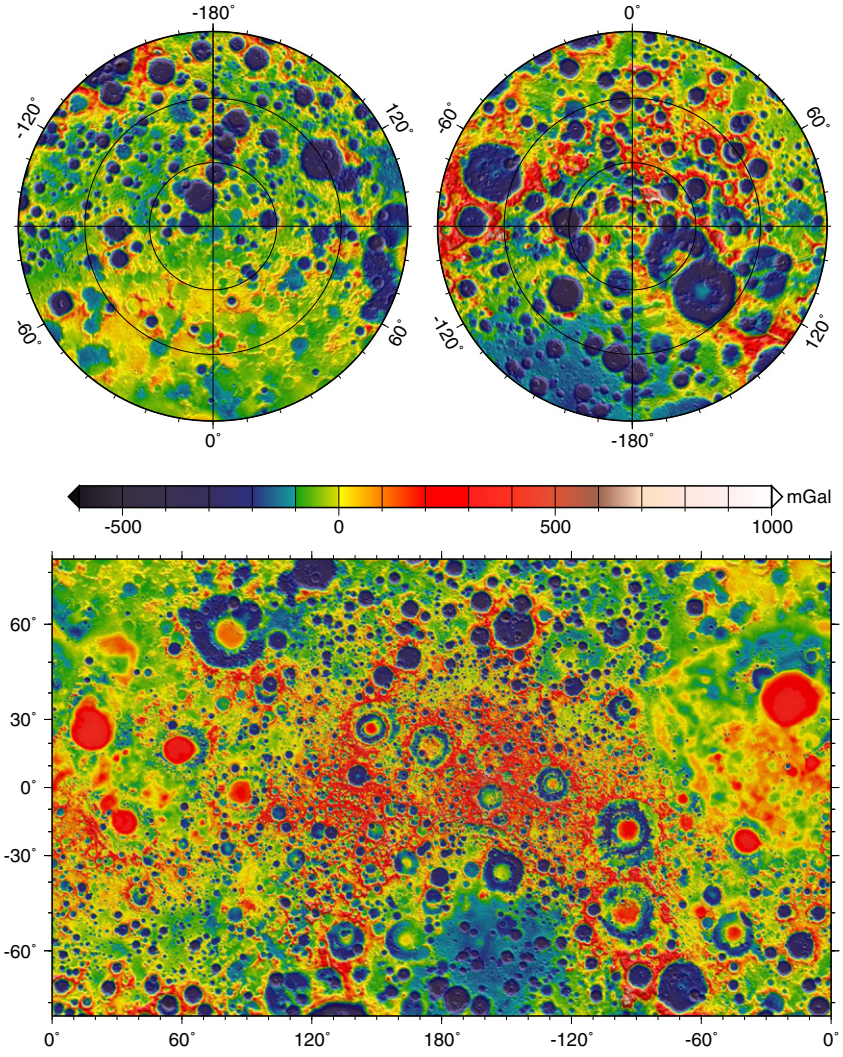

Fig. 8. Gravity anomaly GL0420A (Zuber et al., 2013b) from the 2012 GRAIL primary mission, relative to normal acceleration on a reference sphere of radius 1738 km. Same projection as in Fig. 7.

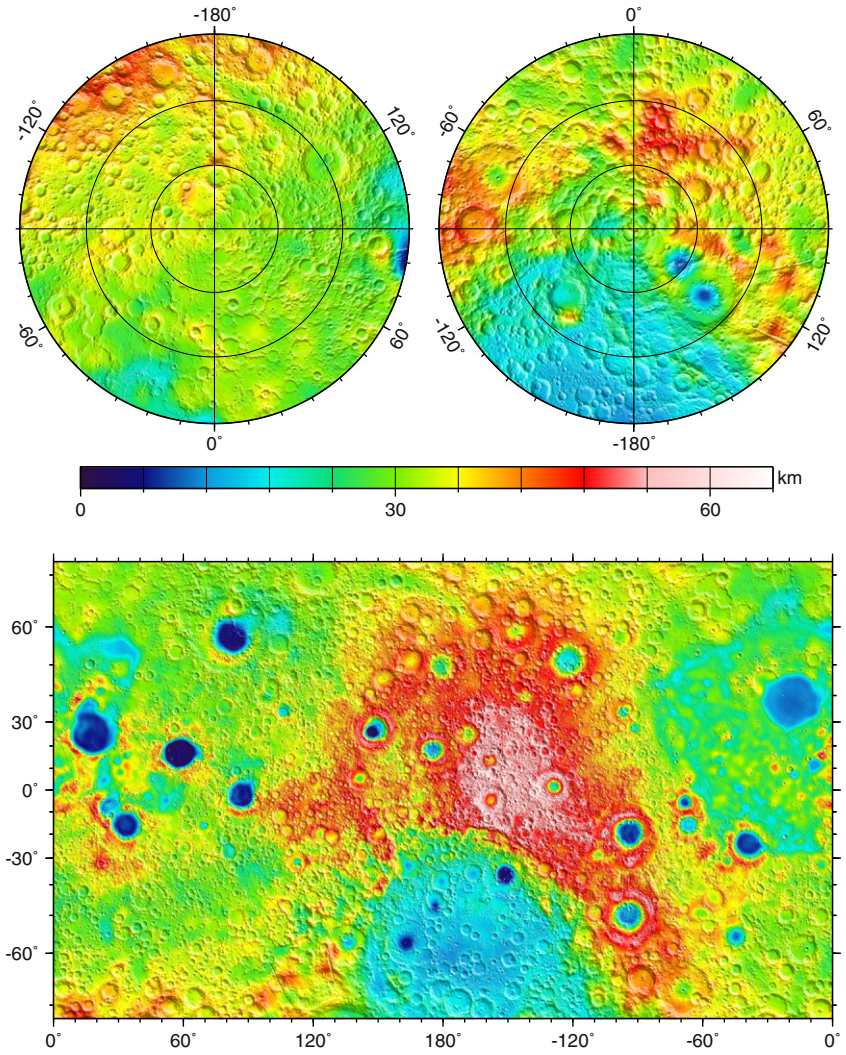

Fig. 9. Crustal thickness from inversion of GL0420A gravity anomaly to degree and order 310 with noise reduction filter amplitude set to 0.5 at degree 80. Same projection as in Fig. 7.

relation (Huang and Wieczorek, 2012). Combined with bulk density estimates, this relation would imply near-surface porosities of 4–21%. Recent studies of bulk and grain density of meteorite and Apollo samples (Kiefer et al., 2012) have placed further constraints on the extent of mechanical and compositional variation of the crust. For a given mineral composition the mechanical brecciation and comminution of crust has a significant effect on density in lunar samples. Excluding mare basalts, Kiefer et al. (2012) found that porosity of crustal samples ranges from 15 to 25%.

Wieczorek et al. (2013) argued that substantial porosity extends in some regions to great depths within the lunar regolith and possibly into the uppermost mantle. Thus Wieczorek et al. (2013) could jointly satisfy a seismically determined thickness of 30–38 km near the Apollo 12 and 14 landing sites by assuming mantle densities of 3150–3320 kg/m^3. These densities would also imply porosities of up to 6% in the uppermost mantle relative to an assumed grain density of 3360 kg/m^3.

The minimum crustal thickness of 45 km at Apollo 12 derived by Ishihara et al. (2009) can now be revised downward in the light of reanalysis of lunar sample bulk densities, and with refined gravity data from the GRAIL mission. The chief justification for such a revision is the recognition that the bulk porosity of the lunar megaregolith is higher than previously assumed consistent with lunar sample measurements, localized admittances and the latest results obtained by GRAIL. The higher porosity and lower density imply a greater density contrast at the Moho. Ishihara et al. (2009) assumed a uniform density single-layer crust with density $\rho_c = 2800$ kg/m^3, based primarily on mineralogical estimates, and a density contrast at the Moho of 560 kg/m^3. The greater density contrast at the Moho (770 kg/m^3) permits models (Fig. 9) with a crustal thickness of 30 and 32.5 km at the Apollo 12/14 sites, using a mean crustal thickness of 35.25 km. The minimum thicknesses of 0.05 km at Moscoviense, 3 km at Crisium, and 5 km at Humboldtianum imply some excavation of mantle material, while the model implies a maximum crustal thickness of at least 68 km on the farside. This model illustrates the feasibility of constructing global crustal thickness models consistent with the recent seismological results (Gagnepain-Beyneix et al., 2006; Khan and Mosegaard, 2002; Khan et al., 2000; Lognonné et al., 2003).

5. Constraints on lunar composition and implications for lunar origin and evolution

5.1. Petrological context

Since the analysis of the returned Apollo samples, there is widespread belief that the Moon underwent a large-scale melting process referred to as the Lunar Magma Ocean (LMO) (e.g., Smith et al., 1970; Wood et al., 1970). The crystallization of the LMO is the source of most of the rocks that compose the lunar crust, in particular the low-density plagioclase-rich crust originated by crystallization and

subsequent flotation in a magma ocean (e.g. Warren, 1985). An anorthositic crust containing ~25 wt.% Al_2O_3, with a density of about 2950 kg/m^3 (excluding porosity), is thought to be representative of the lunar highland crust (e.g., Taylor, 1982). Such a thick highland crust of plagioclase feldspar, requires a Moon with a substantial refractory element content (e.g., Taylor et al., 2006). This constraint is of course critically dependent upon both the thickness of the crust and its abundance of anorthosite. The lunar upper anorthositic crust consists of 82–100 vol.% plagioclase (e.g. Korotev et al., 2010; Ohtake et al., 2009; Warren, 1990, 2005) and anorthositic gabbro, while the proportion of plagioclase in the lower crust is estimated to be ~65 vol.%, whose overall composition is thought to be more mafic (e.g., Wieczorek et al., 2006) (see Fig. 10). Compositionally distinct upper and lower crustal materials are favored on the basis of several field observations that imply noritic compositions of basin ejecta, central peaks as well as material within the floor of the South Pole-Aitken basin (e.g., Cahill et al., 2009; Davis and Spudis, 1985; Lucey et al., 1995; Spudis et al., 1984; Tompkins and Pieters, 1999; Wieczorek and Zuber, 2001). A recent estimate by Wieczorek and Zuber (2001) gives 29–32, 24–29 and 18–25 wt.% Al_2O_3 for the upper, lower and most mafic lower crust, respectively. Assuming that the upper and lower crusts are equal in volume, this leads to an average crustal Al_2O_3 content of 28.5 wt.% (Wieczorek and Zuber, 2001) compared to the earlier estimate of 24.6 wt.% (Taylor, 1982). In light of the results from GRAIL these estimates are likely to be refined.

Rocks that were produced during post-LMO crystallization magmatism include mare basalts and rocks from the alkali-, and magnesian-suites. Several models of LMO crystallization and differentiation have been proposed in order to explain the present-day chemical composition and physical structure of the Moon (e.g. Elardo et al., 2011; Longhi, 1980, 2003; Snyder et al., 1992; Tonks and Melosh, 1990). A simple schematic cross section of the resulting lithologies of the lunar crust and upper mantle is presented in Fig. 10. Different estimates of the bulk LMO composition (O'Neill, 1991; Taylor, 1982) underlined that plagioclase saturated after 73% (±5%) of dunite and pyroxenite fractionation and that ilmenite precipitated after 95% crystallization of olivine + pyroxene + plagioclase (e.g. Longhi, 2003). During crystallization, the residual liquids were enriched in incompatible trace elements that were excluded from the crystal structures of olivine, pyroxenes and plagioclase. These elements are K, REE, P ("KREEP"), Th, U, Zr, Hf and Nb. As argued by Shearer and Papike (1999), a large part of this KREEP component was probably later integrated into the feldspathic highland crust.

Fig. 10 also highlights the likely repartition of plagioclase, which is a critical part of our understanding of the crystallization of the magma ocean and the early evolution of the lunar crust. It has been long thought that the anorthositic crust involved the separation and flotation of plagioclase to the top of the LMO, while denser mafic minerals sunk to the bottom of the magma ocean (Snyder et al., 1992; Taylor, 1982; Wood et al., 1970). However, recent studies (Cahill et al., 2009; Wieczorek and Zuber, 2001) have suggested that this process was probably less efficient than previously thought, since the middle and lower parts of the layered lunar crust can contain up to 50 wt.% plagioclase. As recently suggested by Namur et al. (2011), a likely explanation is to interpret the significant presence of plagioclase in the lower crust as the consequence of either the low efficiency of plagioclase extraction from basal cumulates or the low efficiency of crystal nucleation from the main magma body. Based on comparisons with anorthositic-rich layered intrusions in the Earth, the same authors support the hypothesis of a formation of ferroan anorthosites in the upper crust by plagioclase flotation, while the noritic lower crust possibly results from in-situ fractional crystallization at the base of the LMO.

An important compositional aspect of the lunar interior concerns ilmenite cumulates. Ilmenite is the last phase to crystallize out of the magma ocean. It is generally thought that these ilmenite-bearing cumulates were grouped into a thin layer at the base of the crust, and, being denser than the surrounding mantle, would sink to the deep interior as a result of gravitational instability, possibly transformed into other stable high-Ti phases at depths of less than 280 km (Thacker et al., 2009). This latter stage of LMO crystallization is known as cumulate-pile overturn (Elkins-Tanton et al., 2002; Hess and Parmentier, 1995; Shearer and Papike, 1999; Shearer et al., 2006). Various overturn models suggest that cumulates, because of an upward progressive enrichment in FeO, and accompanying increase in density, would lead to a gravitationally unstable sequence (cumulate pile) (e.g. Elkins-Tanton et al., 2011; Shearer and Papike, 1999). Moreover, as ilmenite cumulates likely also integrated heat-producing elements (U, Th, REE, K, Rb), they might be responsible for having initiated melting at depth (e.g. Shearer et al., 1991) producing buoyantly stable TiO_2-rich melts in the deep lunar interior (e.g., Delano, 1990; Sakamaki et al., 2010; van Kan Parker et al., 2012), thereby providing an explanation for the presence of deep-seated partial melt as observed geophysically (e.g., Nakamura et al., 1973; Weber et al., 2010; Williams et al., 2001). In the context of a deep melt layer, we would like to note that Nimmo et al. (2012) have recently shown that a melt-free viscoelastically dissipating Moon, based on an extended Burgers

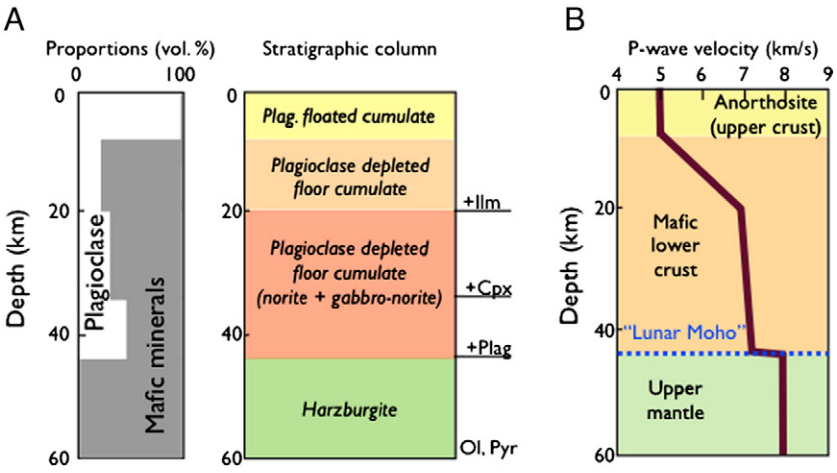

Fig. 10. Composition of the lunar crust and upper mantle. A) Mineralogy and stratigraphic column, with relative proportions of plagioclase and mafic minerals (left) and a possible sequence of crystallization (right) (after Namur et al. (2011). B) Comparison with seismic P-wave velocity structure, averaged from Khan et al. (2000). The good correlation between seismic wave velocity and compositional layering highlights the importance of seismic studies as part of the investigation of the mineralogy and structure of the Moon. See text for details.

model, is also compatible with observed dissipation at both tidal and seismic frequencies.

The idea of mantle overturn is not new and various models have been proposed attributing variable efficiency to this process (Hess and Parmentier, 1995; Shearer et al., 1996; Snyder et al., 1992; Spera, 1992). However, it seems that a large-scale overturn is required to explain numerous chemical and mineralogical signatures, such as the KREEP component in primitive magmas (e.g., Shearer and Papike, 1999). It is also interesting to consider the possible impact of ilmenite cumulates on the fate of plagioclase cumulates inside the crystallizing crust. In case ilmenite-saturated melts are denser than plagioclase, the flotation process would be enhanced, increasing the thickness of the anorthositic layer. On the other hand, denser plagioclase cumulates would stop the flotation process and part of them would sink, explaining their presence in the lower crust (e.g., Namur et al., 2011).

The lunar upper mantle is ultramafic in composition. It was likely produced during the crystallization of the LMO and is thought to consist of deep cumulate rocks. As there is no outcrop of these rocks on the Moon, their petrological properties are investigated from their products of partial melting (mare basalts) (Head and Wilson, 1992; Longhi, 2006). The lunar upper mantle is thought to be rather homogenous in composition, although this does not exclude the presence of heterogeneities related to mineral phase transformations. Indeed, as recently suggested by Thacker et al. (2009), the phase transformation of ilmenite-bearing cumulate to a higher-pressure phase (armalcolite) that may have occurred during the cumulate overturn process would have been accompanied with only a small increase in density. As a consequence, Thacker et al. deduce that ilmenite sinking may have been less efficient than previously thought and suggest that such a phase transformation may have increased the chance of preservation of armalcolite-bearing pockets in the upper mantle.

5.2. Are the Earth and Moon compositionally alike?

Using seismology as a means to infer the composition of the lunar interior has been the subject of several studies with the intent of providing constraints on lunar formation and evolution. The initial work of Buck et al. (1980), Hood and Jones (1987), and Mueller et al. (1988) were limited to comparing Apollo-era derived seismic velocity models to those expected from a restricted suite of mantle mineral assemblages, while later studies (e.g., Khan et al., 2006a,b, 2007; Kronrod and Kuskov, 2011; Kuskov and Kronrod, 1998, 2001, 2009; Kuskov et al., 2002) considered a more elaborate thermodynamic approach based on Gibbs free energy minimization techniques. Interfacing the latter with the stochastic-based inversion scheme employed previously, Khan et al. (2006a) computed stable mineral phases as a function of temperature and pressure, their modes and physical properties (P-, S-wave velocity and density) within the CFMAS system (comprising oxides of the elements $CaO-FeO-MgO-Al_2O_3-SiO_2$). By inverting the seismic travel time data set of LG03 jointly with lunar mass and moment of inertia, while assuming crust and mantle to be compositionally uniform, they determined the compositional range of the oxide elements, thermal state, Mg#, mineralogy and physical structure of the lunar interior, as well as constraining core size and density (for details the reader is referred to Khan et al. (2007)).

The crustal compositions retrieved in this study showed Al_2O_3 contents in the range of 24–26 wt.% and thus slightly lower than the recent determination by Wieczorek and Zuber (2001), but in overall agreement with the crustal composition of Taylor and Jakes (1974). If the new crustal thickness value of 30–45 km beneath Apollo stations 12 and 14 (Khan et al., 2000; Lognonné et al., 2003), making up 7.6% of lunar volume, is extrapolated globally, an average thickness of around 52 km is found (Wieczorek, 2003), comprising about 8.7% of lunar volume. If it is assumed that the plagioclase-rich part of the crust extends to 30 km depth (Wieczorek and Zuber, 2001), decreasing crustal thickness will increase the relative proportions of the upper Al_2O_3-rich crust. However, if the crust is derived from a smaller volume of the Moon, then an increased bulk-Moon abundance of Al_2O_3 is required. Although this implies that crustal composition and thickness can be used to place constraints on the lunar bulk aluminum content, the latter is primarily determined by the amount of alumina residing in the mantle as discussed in detail by Wieczorek et al. (2006).

Additional evidence in favor of the geophysically-derived crustal compositions exists in the form of empirically-determined elemental abundance correlations. These can be used to determine FeO/MgO and MgO/SiO_2 ratios, from which a representative lunar surface Mg# is derivable. Warren (1986), for example, advocates a Mg# of 68 for the uppermost lunar crust based on various soil compositions and lunar meteorites. Lower crustal components represented by the low-K Fra Mauro basalts indicate a Mg# of 70 ± 3 (e.g., Ryder and Spudis, 1987). While these values do not directly indicate a varying crustal composition as a function of depth, there is evidence for the latter, as ejecta from basin forming impacts is observed to be more noritic as observed above. The crustal Mg#s obtained from the inversion are ~66 in general agreement with sample-based observations ranging from 65 to 68 (e.g., Demidova et al., 2007; Korotev, 1997; Korotev et al., 2003; Palme et al., 1991).

The geophysically-determined mineralogy of Khan et al. (2006a) indicates a lunar mantle mineralogy that is dominated by olivine and orthopyroxene (~80 vol.%), with the remainder being composed of clinopyroxene and an aluminous phase present as plagioclase, spinel, and garnet in the depth ranges of 0–150 km, 150–200 and200 km, respectively (Fig. 11), in agreement with recent independent estimates based also on geophysical–thermodynamical modeling (e.g., Kronrod and Kuskov, 2011; Kuskov and Kronrod, 2009). The corresponding P- and S-wave velocity models are relatively smooth with no major velocity changes occuring. This is clearly discernible in Fig. 11. The small variations observable in both P- and S-wave profiles though, are due to effects of increasing pressures and temperatures, with the latter being most significant because of the small pressures prevalent in the Moon (~4 GPa in the centre). P-wave velocity increases slightly as a function of depth as a result of an increased amount of the higher velocity phase garnet, which is also reflected in the density profiles (not shown for brevity), while S-wave velocity decreases as it is relatively more sensitive to temperature than P-wave velocity. The apparently uniform mantle is suggestive of extensive stirring and homogenization by convection as part of early lunar evolution, possibly during the period when the magma ocean was present. The lunar temperature profiles (not shown) determined thermodynamically agree with subsolidus conditions throughout the entire depth range of the mantle. At 1000 km depth temperatures are found to lie in the range of 1000–1350 °C, with a further small increase toward the bottom of the mantle to 1150–1500 °C (e.g., Hood et al., 1982b; Khan et al., 2006a, 2006b; Kuskov and Kronrod, 2009; Pullan and Lambeck, 1980).

The presence of garnet in the lower mantle implies the presence of Al_2O_3 and several attempts have been made to estimate the bulk aluminum content of the Moon using various assumptions, e.g., Taylor (1982): 1) an average crustal Al_2O_3 content of 24.6 wt.%, 2) the Apollo-era crustal thickness value of 61 km, which amounts to 10% of lunar volume, 3) whole-Moon melting, and 4) a reasonable assumption of the distribution of Al in the interior of the Moon. Based on this Taylor obtained an estimate of the Al_2O_3 content for the bulk Moon to be 6 wt.%. Similar values have been obtained elsewhere, e.g., in the thermodynamic approach of Kuskov and Kronrod (1998) and more recently by Kuskov and Kronrod (2009) and Kronrod and Kuskov (2011), who inferred lunar mantle composition (in the system CFMASNaTi, with Na_2O and TiO_2 fixed to chondritic values) using Apollo-era seismic model NK83, as well as studies based on mass-balance calculations relying on remote sensing data of the lunar surface (e.g., Jolliff et al., 2000). In contrast to this, more Earth-like refractory element abundances have been obtained by e.g., Warren and Rasmussen (1987) based on revised estimates of globally-averaged lunar heat flow data, and Warren (2005), who 1) employed recent lunar meteorite data, 2) recalibrated the global

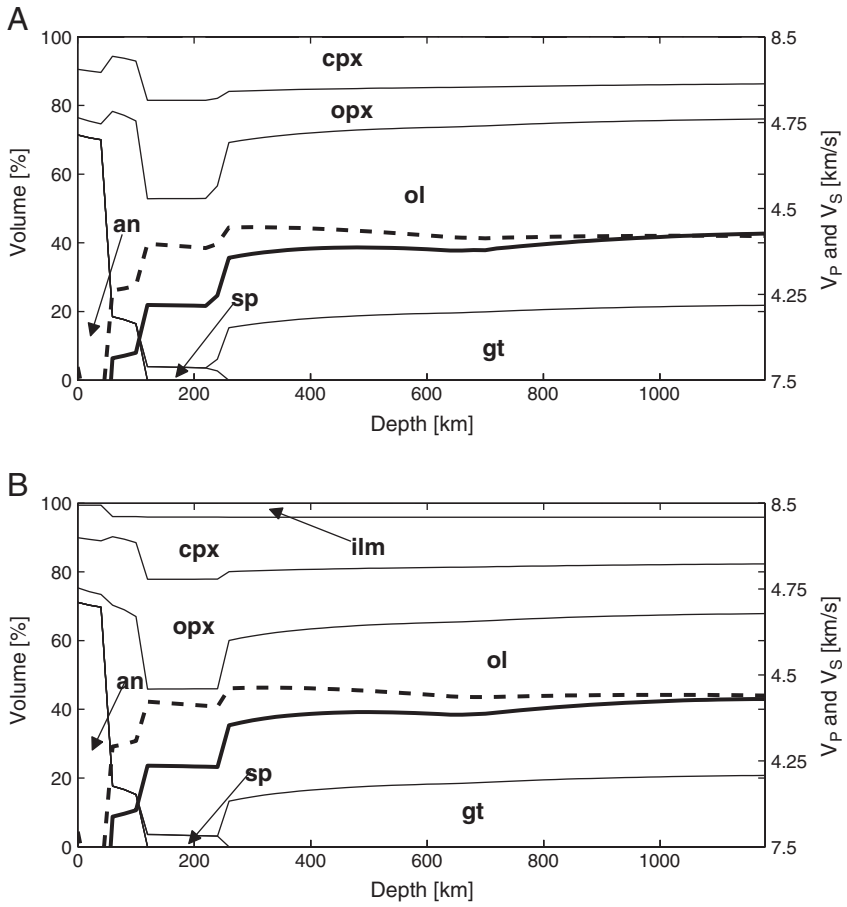

Fig. 11. Example of mineral phase equilibria and seismic velocities (bold solid lines (V_P) and dashed lines (V_S)) as a function of depth (pressure) computed in the CFMAS (A) and CFMASTi (B) systems, respectively. Equilibrium mineralogy is computed on the basis of a typical mantle composition (see Fig. 12) and a lunar temperature profile using Gibbs free energy minimization (see main text for details). In the case of (B) we added 3 wt.% TiO_2 in the mantle (adopted from Khan et al., 2013). Phases are anorthite (an), olivine (ol), orthopyroxene (opx), clinopyroxene (cpx), spinel (sp), garnet (gt), and ilmenite (ilm).

Th data relying on the Lunar Prospector gamma-ray data of Prettyman et al. (2002), and 3) assumed chondritic proportionality among major elements, to find an Al_2O_3 abundance of 3.8 wt.%. For comparison, Khan et al. (2006a), retrieve refractory element abundances akin to those in Earth's upper mantle, i.e., 4–4.5 wt.% Al_2O_3 (e.g., McDonough and Sun, 1995; Taylor, 1980) (see Fig. 12).

The bulk compositions of Khan et al. (2006a) (see Fig. 12) also indicate bulk lunar Mg#s of ~83. This result is generally in agreement with petrological estimates where lunar Mg#s ranging from 75 to 84 have been proposed (e.g., Delano, 1986; Jones and Delano, 1989; Ringwood, 1979; Taylor, 1982) and the general observation that lunar basalts are more FeO-rich (lower Mg#) than terrestrial basalts (Drake, 1986; Wänke and Dreibus, 1986). This value is generally lower than the Mg# of Earth's upper mantle which has been reasonably well estimated at 89 (McDonough and Sun, 1995; Palme and Nickel, 1985; Ringwood, 1979; Taylor, 1980). The geophysical–thermodynamical models of Kuskov and Kronrod (1998, 2009) and Kronrod and Kuskov (2011) likewise suggested bulk lunar Mg#s in the range of 82–84.5. Warren (2005), on the other hand, estimates a bulk Earth-like lunar Mg# of 87–88. Compositional estimates of Earth's upper mantle (e.g., Lyubetskaya and Korenaga, 2007; McDonough and Sun, 1995; Salters & Stracke, 2004) are principally based on studies of the composition of meteorites, mantle xenoliths and the basaltic products of mantle melting and are similar to the pyrolite composition of Ringwood (1966). In contrast, the results of Khan et al. (2006a) imply mantle compositions for the Moon (Fig. 12) that are unlike that of pyrolite, in that these models have higher FeO, lower MgO, and lower refractory element contents relative to pyrolite, in general agreement with other lunar literature estimates. This suggests compositional differences between Earth and Moon, reflecting different evolutionary histories of their respective (upper) mantles.

It has to be remarked, however, that the results of Khan et al. are based on the assumption of a compositionally uniform mantle, while also being restricted in terms of chemical components (neglect of TiO_2), due to a lack of appropriate thermodynamic data. In the first place, a mid-mantle seismic discontinuity that separates upper from lower mantle, although present in all lunar seismic models shown in Fig. 5, is yet to be established. Khan et al., for example, found that uniform mantle models, which effectively rule out the presence of mantle seismic discontinuities (see Fig. 11), provide an adequate fit to the seismic travel time data set. Thus, while this argues that mid-mantle discontinuities are not well-constrained, it does not rule them out. Indeed, if the LMO event only encompassed half of the Moon to a depth of 500–700 km, a discontinuity separating an upper differentiated mantle from a lower, possibly, pristine mantle composition would potentially be envisaged (e.g., Hood and Jones, 1987). However, given that the depth of the LMO is not well established, with scenarios ranging from shallow depth (200 km depth) (e.g., Solomon and Chaiken, 1976), over mid-mantle (e.g., Elkins-Tanton et al., 2011; Neal, 2001; Wieczorek and Phillips, 2000) to whole-Moon involvement (e.g., Taylor, 1986), any connection between the two is speculative at best and will have to be left for future studies considering expanded and/or new data sets.

Secondly, as some mare basalts have been observed to contain up to 14 wt.% TiO_2, while lunar picritic glass beads, which are representative of the most primitive lunar magmas yet sampled, vary broadly

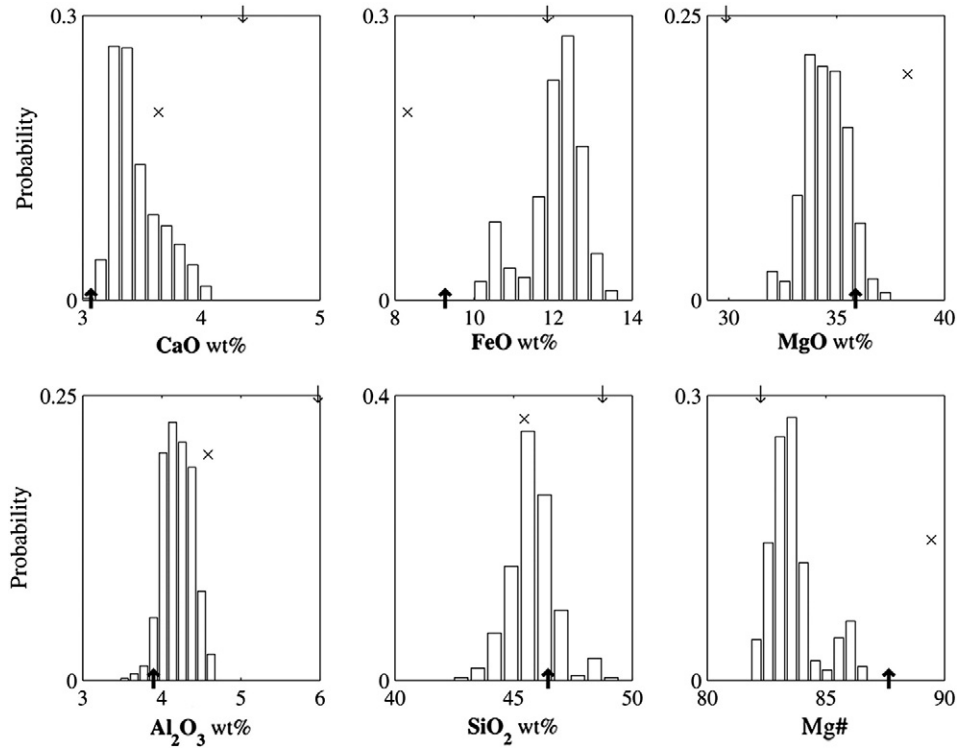

Fig. 12. Bulk lunar silicate composition in wt%. Histograms depict sampled marginal posterior probability density distributions of CaO, FeO, MgO, Al_2O_3, SiO_2, and Mg#s. Upward and downward pointing arrows show bulk compositional estimates of Warren (2005) and Kuskov and Kronrod (1998), respectively, while crosses denote bulk composition of the Earth's upper mantle (McDonough and Sun, 1995). Used by permission of the American Geophysical Union, from Khan et al. (2006a), Journal of Geophysical Research, Vol. 111, Fig. 8, p. 17.

in titanium content (up to 16.4 wt.% TiO_2) (e.g., Delano, 1986, 1990), a potential problem with the thermodynamic-based studies of e.g., Khan et al. (2006a) and Kuskov et al. (2002) is the neglect of titanium-rich phases in the form of ilmenite. This should also be considered in the light of recent laboratory studies on high-TiO_2 basalt melt and magma (e.g., Sakamaki et al., 2010; van Kan Parker et al., 2012) that indicate that solidified high-Ti basalt components and potentially also melts are stable in the lunar interior thereby giving rise to chemical heterogeneities accompanied by seismic velocity and density anomalies. However, current geophysical-thermodynamic modeling using an expanded thermodynamic database that includes titanium-rich phases indicates insignificant changes to physical properties (cf. figures 11A and 11B). It might be noted that to substantiate their compositional models found, Khan et al. (2006a) observed that by melting a typical model mantle composition using the pMELTS algorithm (Ghiorso et al., 2002), a range of batch melts generated from these models have features in common with low-Ti mare basalts and picritic glasses. These calculations showed that 1) their model is broadly consistent with constraints on mantle mineralogy derived from the experimental and observational study of the phase relationships and trace element compositions of lunar mare basalts and picritic glasses, and 2) that the experimental work on the low-Ti lunar mare basalt and picrite glasses cannot be used as a means of discounting their preferred lunar mantle composition recovered. In spite of this, it is clear that large uncertainties remain and we will have to leave it to future studies using expanded and improved data (e.g., seismic, thermodynamic, petrological) to refine present results.

6. Concluding remarks and future prospects

As this review has shown study of the lunar interior using the seismic data gathered in the 1970s continues to this day and will do so until new data are acquired. From the beginning the Apollo lunar seismic experiment was compromised in the limitations it faced. Of most importance in this regard (see also Nakamura, 2010) were limitations on spatial extent of the network, relatively short duration of network operation, number of stations available, bandwidth, and not least the complex signals characteristics, which up until now has strongly limited the amount of usable information that could be extracted from the lunar seismic signals. In spite of these limitations the Apollo lunar seismic data nonetheless represent a unique resource that has enabled us, and continues to do so, to study the internal structure of a planetary body besides Earth. However, as details of lunar internal structure remain rudimentary continued analysis of the data set is warranted, including those parts of the data that have not yet been analyzed in detail, particularly the data recorded by the short period instruments (Nakamura, 2010). While significant improvement of our understanding of the deep lunar interior will likely only come with the acquisition of new high-quality seismic data, a very important step forward would be the positive identification of refracted and particularly reflected phases off of seismic velocity discontinuities currently buried in the seismic coda. This Gordian knot has so far proven very difficult to solve and although recent attempts at retrieving core-reflected phases have shown some promise (e.g., Garcia et al., 2011; Weber et al., 2010), unambiguous confirmation of the purported findings is yet to be firmly established.

Global-scale issues that remain to be resolved from a geophysical point of view include

- crustal structure, including presence and nature of intra-crustal layering,
- resolving mantle discontinuities and their relationship to the LMO event.
- size and state of a putative lunar core.
- and not least, the question of lateral variations in crust and mantle structure.

This list is by no means exhaustive and the reader is referred to e.g., Wieczorek et al. (2006) and Neal (2009) for discussion of other aspects. A couple of further comments can be made.

First of all, obtaining better estimates of the thickness of the anorthosite layer would help place important constraints on the differentiation

path of the lunar magma ocean, including the question of the efficiency of plagioclase flotation. Thickness estimates of the anorthosite layer presently range from a few km to up to 20 km (Longhi, 1982; Ohtake et al., 2009; Wood, 1986), whereas recent petrological considerations that are based on similarities with terrestrial anorthosites, suggest a anorthosite layer around 8 km thick (Namur et al., 2011).

Secondly, laboratory experiments continue to improve our knowledge of mineral physics data (e.g., Sakamaki et al., 2010; van Kan Parker et al., 2012), which can be applied in geophysical modeling and studies of the lunar interior (e.g., Khan et al., 2006a,b; Kuskov and Kronrod, 2009; Kuskov et al., 2002). Construction of accurate models of the physico-chemical structure would help to differentiate between various models of lunar evolution. For instance, the determination of stability fields and element partitioning of ilmenite cumulates (Thacker et al., 2009) are a critical part of our understanding of the efficiency of mantle overturn. Based on density considerations regarding ilmenite and its high-pressure polymorph armalcolite, it is suggested that armalcolite-bearing pockets were possibly preserved in the lunar upper mantle. If such bodies were to be detected through future geophysical measurements, then our current view of the mantle overturn process as well as its efficiency, and therefore of late-stage lunar evolution, would be significantly modified and improved.

Third, as reviewed by e.g., Williams et al. (2001), Khan et al. (2004) and Wieczorek et al. (2006) among others, several lines of evidence, such as lunar laser ranging-based studies (Khan and Mosegaard, 2005; Khan et al., 2004; Williams et al., 2001), moment of inertia (Konopliv et al., 1998), induced magnetic dipole moment (Hood et al., 1999), depletion of highly siderophile elements in the mare basalt source region (Righter, 2002), remanent magnetism in lunar rocks (e.g., Hood, 1995), geophysical–thermodynamical modeling (Khan et al., 2006a; Kronrod and Kuskov, 2011; Kuskov and Kronrod, 2009), and tentative evidence for core reflected phases (Garcia et al., 2011; Weber et al., 2010) have independently hinted at the existence of a small lunar core of pure Fe or Fe–S (the alloying element is not known) <450 km in radius, making up 1–4% of lunar mass, in accordance with predictions from the giant impact model. However, this will have to be corroborated through continued analysis of lunar laser ranging data (Williams et al., 2012) and, if possible, the Apollo lunar seismic data.

Until then we will have to await the future emplacement of seismometers on the Moon. To improve upon the lessons learned from the Apollo missions, requirements for a lunar seismic network should include seismic station arrays on a global, regional, and preferably also local scale in order to map out small-scale as well as large-scale lateral variations. Of equal importance will be the deployment of broadband instruments sensitive enough to resolve the seismic background noise level (e.g., Lognonné et al., 2009) as well as normal modes. For a summary of future missions to the Moon, their concepts and scientific goals see e.g., Neal (2009), Mimoun et al. (2011) and Yamada et al. (2011).

Acknowledgments

We are grateful to Yosio Nakamura for his thorough comments that helped improve the manuscript. Reviews by O. Kuskov and P. Lognonné were also very helpful. This work was supported by Swiss National Science Foundation grant 200021-130411.

References

Anderson, D.L., Miller, W.F., Latham, G.V., Nakamura, Y., Toksoz, M.N., Dainty, A.M., Duennebier, F.K., Lazarewicz, A.R., Kovach, R.L., Knight, T.C.D., 1977. Seismology on Mars. Journal of Geophysical Research 82, 4524.

Araki, H., Tazawa, S., Noda, H., Ishihara, Y., Goossens, S., Sasaki, S., Kawano, N., Kamiya, I., Otake, H., Oberst, J., Shum, C., 2009. Lunar global shape and polar topography derived from Kaguya-LALT laser altimetry. Science 323, 897. http://dx.doi.org/10.1126/science.1164146.

Archinal, B.A., Rosiek, M.R., Kirk, R.L., Redding, B.L., 2006. Unified Lunar Control Network 2005 Open File Report. U.S. Geological Survey, 2006-1367, Flagstaff, Arizona.

Banerdt, W.B., Chui, T., Herrin, E.T., Rosenbaum, D., Teplitz, V.L., 2006. Lunar seismic search for strange quark matter. Advances in Space Research 37, 1889. http://dx.doi.org/10.1016/j.asr.2005.06.034.

Buck, W.R., Toksöz, M.N., 1980. The bulk composition of the Moon based on geophysical constraints. Proceedings of Lunar and Planetary Science Conference 11th, 2043.

Bulow, R.C., Johnson, C.L., Shearer, P.M., 2005. New events discovered in the Apollo lunar seismic data. Journal of Geophysical Research 110, E10003. http://dx.doi.org/10.1029/2005JE002414.

Bulow, R., Johnson, C.L., Bills, B.G., Shearer, P.M., 2007. Temporal and spatial properties of some deep moonquake clusters. Journal of Geophysical Research Planets 112. http://dx.doi.org/10.1029/2006JE002847.

Cahill, J.T., Lucey, P.G., Wieczorek, M.A., 2009. Compositional variations of the lunar crust: results from radiative transfer modeling of central peak spectra. Journal of Geophysical Research 114, E09001.

Cameron, A.G.W., 2000. Higher resolution simulations of the giant impact. In: Canup, R.M., Righter, K. (Eds.), Origin of the Earth and Moon. Arizona University Press, Arizona, p. 133.

Cameron, A.G.W., Benz, W., 1991. The origin of the Moon and the single impact hypothesis IV. Icarus 92, 204.

Canup, R.M., 2004. Simulations of a late lunar forming impact. Icarus 168, 433.

Canup, R.M., Asphaug, E., 2001. Origin of the Moon in a giant impact near the end of the Earth's formation. Nature 412, 708.

Chenet, H., Lognonné, P., Wieczorek, M.A., Mizutani, H., 2006. Lateral variations of lunar crustal thickness from the Apollo seismic data set. Earth and Planetary Science Letters 243, 1.

Cheng, H.C., Toksöz, M.N., 1978. Tidal streses in the Moon. Journal of Geophysical Research 83, 845.

Cooper, M.R., Kovach, R.L., Watkins, J.S., 1974. Lunar near-surface structure. Reviews of Geophysics and Space Physics 12, 291.

Davis, P.A., Spudis, P.D., 1985. Petrologic province maps of the lunar highlands derived from orbital geochemical data. Proceedings of Lunar and Planetary Science Conference 16th, Part 1Journal of Geophysical Research 90, D61 (Suppl.).

Delano, J.W., 1986. Pristine lunar glasses; criteria, data, and implications. Proceedings of Lunar Planetary Science Conference 13thJournal of Geophysical Research 91, D201.

Delano, J.W., 1990. Buoyancy-driven melt segregation in the Earth's Moon, I: Numerical results. Proceedings of Lunar Planetary Science Conference 20th, 3.

Demidova, S.I., Nazarov, M.A., Lorenz, C.A., Kurat, G., Brandstätter, F., Ntaflos, Th., 2007. Chemical composition of lunar meteorites and the lunar crust. Petrology 15, 386.

Dickey, J.O., Bender, P.L., Faller, J.E., Newhall, X.X., Ricklefs, R.L., Ries, J.G., Shelus, P.J., Veillet, C., Whipple, A.L., Wiant, J.R., Williams, J.G., Yoder, C.F., 1994. Lunar laser ranging: a continuing legacy of the Apollo program. Science 265, 482.

Drake, M.J., 1986. Is lunar bulk composition similar to Earth's mantle? In: Hartmann, W.K., Phillips, R.J., Taylor, G.J. (Eds.), Origin of the Moon. Lunar and Planetary Institute, Houston, TX, p. 105.

Duennebier, F., Sutton, G., 1974. Thermal moonquakes. Journal of Geophysical Research 79, 4351.

Duennebier, F.K., Nakamura, Y., Latham, G.V., Dorman, H.J., 1976. Meteoroid storms detected on the Moon. Science 192, 1000.

Elardo, S.M., Draper, D.S., Shearer Jr., C.K., 2011. Lunar magma ocean crystallization revisited: bulk composition, early cumulate mineralogy, and the source regions of the highlands Mg-suite. Geochimica et Cosmochimica Acta 75, 3024–3045.

Elkins-Tanton, L.T., Van Orman, J., Hager, B.H., Grove, T.L., 2002. Reexamination of the lunar magma ocean cumulate overturn hypothesis: melting or mixing is required. Earth and Planetary Science Letters 196, 249.

Elkins-Tanton, L.T., Burgess, S., Yin, Q.-Z., 2011. The lunar magma ocean: reconciling the solidification process with lunar petrology and geochronology. Earth and Planetary Science Letters 304. http://dx.doi.org/10.1016/j.epsl.2011.02.004.

Frohlich, C., Nakamura, Y., 2006. Possible extra-solar-system cause for certain lunar seismic events. Icarus 185, 21.

Frohlich, C., Nakamura, Y., 2009. The physical mechanisms of deep moonquakes and intermediate-depth earthquakes: how similar and how different? Physics of the Earth and Planetary Interiors 173, 365.

Gagnepain-Beyneix, J., Chenet, H., Lognonné, Lombardi, D., Spohn, T., 2006. A seismic model of the lunar mantle and constraints on temperature and mineralogy. Physics of the Earth and Planetary Interiors 159, 140.

Garcia, R.F., Gagnepain-Beyneix, J., Chevrot, S., Lognonné, P., 2011. Very preliminary reference Moon model. Physics of the Earth and Planetary Interiors 188. http://dx.doi.org/10.1016/j.pepi.2011.06.015.

Garcia, R.F., Gagnepain-Beyneix, J., Chevrot, S., Lognonné, P., 2012. Erratum to "Very preliminary reference Moon model", [Phys. Earth Planet. Inter. 188 (2011) 96–113]. Physics of the Earth and Planetary Interiors 202–203. http://dx.doi.org/10.1016/j.pepi.2012.03.009.

Ghiorso, M.S., Hirschmann, M.M., Reiners, P.W., Kress, V.C., 2002. The pMELTS: a revision of MELTS for improved calculation of phase relations and major element partitioning related to partial melting of the mantle to 3 GPa. Geochemistry, Geophysics, Geosystems 3 (5), 1030. http://dx.doi.org/10.1029/2001GC000217.

Goins, N., Dainty, A., Toksöz, M., 1981a. Seismic energy release of the Moon. Journal of Geophysical Research 86, 378.

Goins, N., Dainty, A., Toksöz, M., 1981b. Lunar seismology: the internal structure of the Moon. Journal of Geophysical Research 86, 5061.

Goins, N.R., Dainty, A.M., Toksöz, M.N., 1981c. Structure of the lunar crust at highland site Apollo station 16. Geophysical Research Letters 8, 29.

Goossens, S.J., Koji Matsumoto, K., Kikuchi, F., Liu, Q., Hanada, H., Lemoine, F.G., Rowlands, D.D., Ishihara, Y., Noda, H., Namiki, N., Iwata, T., Sasaki, S., 2011.

Improved High-Resolution Lunar Gravity Field Model From SELENE and Historical Tracking Data, AGU Fall Meeting, Abstract P44B-05.
Grimm, R.E., Delory, G.T., 2012. Next-generation electromagnetic sounding of the Moon. Advances in Space Research 50, 1687–1701. http://dx.doi.org/10.1016/j.asr.2011.12.014.
Halliday, A.N., Lee, D.C., Jacobsen, S.B., 2000. Tungsten isotopes, the timing of metal-silicate fractionation and the origin of the Earth and Moon. In: Canup, R.M., Righter, K. (Eds.), Origin of the Earth and Moon. University of Arizona Press, Tucson, p. 45.
Han, S.-C., Mazarico, E., Rowlands, D., Lemoine, F., Goossens, S., 2011. New analysis of Lunar Prospector radio tracking data brings the nearside gravity field of the Moon with an unprecedented resolution. Icarus 215, 455. http://dx.doi.org/10.1016/j.icarus.2011.07.020.
Haruyama, J., Ohtake, M., Matsunaga, T., Morota, T., Honda, C., Yokota, Y., Abe, M., Ogawa, Y., Miyamoto, H., Iwasaki, A., et al., 2009. Long-lived volcanism on the lunar farside revealed by SELENE Terrain Camera. Science 323, 905–908.
Head, J.W., Wilson, L., 1992. Lunar mare volcanism: stratigraphy, eruption conditions, and the evolution of secondary crusts. Geochimica et Cosmochimica Acta 56, 2155–2175.
Hess, P.C., Parmentier, E.M., 1995. A model for the thermal and chemical evolution of the Moon's interior: implications for the onset of mare volcanism. Earth and Planetary Science Letters 134, 501–514.
Hikida, H., Wieczorek, M.A., 2007. Crustal thickness of the Moon: new constraints from gravity inversions using polyhedral shape models. Icarus 192. http://dx.doi.org/10.1016/j.icarus.2007.06.015.
Hobbs, B.A., 1977. The electrical conductivity of the moon: an application of inverse theory. Geophysical Journal of the Royal Astronomical Society 51, 727.
Hood, L.L., 1986. Geophysical constraints on the lunar interior. In: Hartmann, W., Phillips, R.J., Taylor, G.J. (Eds.), Origin of the Moon. Lunar and Planetary Institute, Houston, TX, p. 361.
Hood, L.L., 1995. Frozen fields. Earth Moon and Planets 67, 131.
Hood, L.L., Jones, J.H., 1987. Geophysical constraints on lunar bulk composition and structure-A reassessment. Journal of Geophysical Research 92, E396.
Hood, L.L., Sonett, C.P., 1982. Limits on the lunar temperature profile. Geophysical Research Letters 9, 37.
Hood, L.L., Zuber, M.T., 2000. Recent refinements in geophysical constraints on lunar origin and evolution. In: Canup, R.M., Righter, K. (Eds.), Origin of the Earth and Moon. Arizona University Press, Tucson, p. 397.
Hood, L.L., Herbert, F., Sonett, C.P., 1982a. The deep lunar electrical conductivity profile: structural and thermal inferences. Journal of Geophysical Research 87, 5311.
Hood, L.L., Herbert, F., Sonett, C.P., 1982b. Further efforts to limit lunar internal temperatures from electrical conductivity determinations. Journal of Geophysical Research 87, A109.
Hood, L.L., Mitchell, D.L., Lin, R.P., Acuna, M.H., Binder, A.B., 1999. Initial measurements of the lunar-induced magnetic dipole moment using Lunar Prospector magnetometer data. Geophysical Research Letters 26, 2327.
Huang, Q., Wieczorek, M.A., 2012. Density and porosity of the lunar crust from gravity and topography. Journal of Geophysical Research 117, E05003. http://dx.doi.org/10.1029/2012JE004062.
Huebner, J.S., Wiggins, L.B., Duba, A.G., 1979. Electrical conductivity of pyroxene which contains trivalent cations: laboratory measurements and the lunar temperature profile. Journal of Geophysical Research 84, 4652.
Ishihara, Y., Goossens, S., Matsumoto, K., Noda, H., Araki, H., Namiki, N., Hanada, H., Iwata, T., Tazawa, S., Sasaki, S., 2009. Crustal thickness of the Moon: implications for farside basin structures. Geophysical Research Letters 36, L19202. http://dx.doi.org/10.1029/2009GL039708.
Jolliff, B.L., Gillis, J.J., Haskin, L., Korotev, R.L., Wieczorek, M.A., 2000. Major lunar crustal terranes: surface expressions and crust–mantle origins. Journal of Geophysical Research 105, 4197.
Jolliff, B.L., Wieczorek, M.A., Shearer, C.K., Neal, C.R. (Eds.), 2006. New views of the Moon. Reviews of Mineralogy and Geochemistry, 60. Mineralogical Society of America, Chantilly, Virginia (721 pp.).
Jones, J.H., Delano, J.W., 1989. A three-component model for the bulk composition of the Moon. Geochimica et Cosmochimica Acta 53, 513.
Kaula, W.M., Schubert, G., Lingenfelter, R.E., Sjogren, W.L., Wollenhaupt, W.R., 1972. Analysis and interpretation of lunar laser altimetry. Proc. Lunar Planet. Sci. Conf., 3rd, p. 2189.
Khan, A., Mosegaard, K., 2002. An enquiry into the lunar interior—a non-linear inversion of the Apollo lunar seismic data. Journal of Geophysical Research 107. http://dx.doi.org/10.1029/2001JE001658.
Khan, A., Mosegaard, K., 2005. Further constraints on the deep lunar interior. Geophysical Research Letters 32. http://dx.doi.org/10.1029/2005GL023985.
Khan, A., Mosegaard, K., Rasmussen, K.L., 2000. A new seismic velocity model for the Moon from a monte carlo inversion of the Apollo lunar seismic data. Geophysical Research Letters 27, 1591.
Khan, A., Pommier, A., Connolly, J.A.D., 2013. On the presence of a Titanium-rich melt-layer in the deep lunar interior. Lunar and Planetary Science Conference XLIV, abstract 1272. Lunar and Planetary Institute, Houston.
Khan, A., Mosegaard, K., Williams, J.G., Lognonné, P., 2004. Does the Moon possess a molten core? Probing the deep lunar interior using results from LLR and Lunar Prospector. Journal of Geophysical Research 109. http://dx.doi.org/10.1029/2004JE002294.
Khan, A., Maclennan, J., Taylor, S.R., Connolly, J.A.D., 2006a. Are the Earth and the Moon compositionally alike?—Inferences on lunar composition and implications for lunar origin and evolution from geophysical modeling. Journal of Geophysical Research 111. http://dx.doi.org/10.1029/2005JE002608.
Khan, A., Connolly, J.A.D., Olsen, N., Mosegaard, K., 2006b. Constraining the composition and thermal state of the Moon from an inversion of electromagnetic lunar day-side transfer functions. Earth and Planetary Science Letters 248. http://dx.doi.org/10.1016/j.epsl.2006.04.008.
Khan, A., Connolly, J.A.D., Maclennan, J., Mosegaard, K., 2007. Joint inversion of seismic and gravity data for lunar composition and thermal state. Geophysical Journal International 168. http://dx.doi.org/10.1111/j.1365-246X.2006.03200.x.
Kiefer, W.-S., Macke, R.L., Britt, D.T., Irving, A.J., Consolmagno, G.L., 2012. The density and porosity of lunar rocks. Geophysical Research Letters 39 (7). http://dx.doi.org/10.1029/2012GL051319.
Konopliv, A., Binder, A.B., Hood, L.L., Kucinskas, A.B., Sjögren, W.L., Williams, J.G., 1998. Improved gravity field of the Moon from Lunar Prospector. Science 281, 1476.
Konopliv, A.S., Asmar, S.W., Carranza, E., Sjogren, W.L., Yuan, D.N., 2001. Recent gravity models as a result of the Lunar Prospector mission. Icarus 150, 1.
Korotev, R.L., 1997. Some things we can infer about the Moon from the composition of the Apollo 16 regolith. Meteoritics and Planetary Science 32, 447.
Korotev, R.L., Jolliff, B.L., Zeigler, R.A., et al., 2003. Feldspathic lunar meteorites and their implications for compositional remote sensing of the lunar surface and the composition of the lunar crust. Geochimica et Cosmochimica Acta 67, 4895.
Korotev, R.L., Jolliff, B.L., Zeigler, R.A., 2010. On the origin of the Moon's feldspathic highlands, pure anorthosite and the feldsphatic meteorites. Lunar and Planetary Science Conference XLI, abstract 1440. Lunar and Planetary Institute, Houston.
Kovach, R., Watkins, J., 1973a. Apollo 17 seismic profiling-Probing the lunar crust. Science 180, 1063.
Kovach, R., Watkins, J., 1973b. The structure of the lunar crust at the Apollo 17 site. Geochimistry and Cosmochimistry Acta 37 (Suppl. 4), 1549.
Koyama, J., Nakamura, Y., 1980. Focal mechanism of deep moonquakes. Proceedings of Lunar Planetary Science Conference 11th, p. 1855.
Kronrod, V.A., Kuskov, O.L., 2011. Inversion of seismic and gravity data for the composition and core sizes of the Moon. Physics of the Solid Earth 47, 711.
Ksanfomality, L.V., Zubkova, V.M., Morozov, N.A., Petrova, E.V., 1982. Microseisms at the Venera 13 and Venera 14 landing sites. Soviet Astronomical Letters 8, 241.
Kuskov, O.L., Kronrod, V.A., 1998. Constitution of the Moon: 5. Constraints on composition, density, temperature, and radius of a core. Physics of the Earth and Planetary Interiors 107, 285.
Kuskov, O.L., Kronrod, V.A., 2001. Core sizes and internal structure of Earth's and Jupiter's satellites. Icarus 151, 204.
Kuskov, O.L., Kronrod, V.A., 2009. Geochemical constraints on the model of the composition and thermal conditions of the Moon according to seismic data. Physics of the Solid Earth 45, 753.
Kuskov, O.L., Kronrod, V.A., Hood, L.L., 2002. Geochemical constraints on the seismic properties of the lunar mantle. Physics of the Earth and Planetary Interiors 134, 175.
Lammlein, D., 1977. Lunar seismicity and tectonics. Physics of the Earth and Planetary Interiors 14, 224.
Lammlein, D., Latham, G., Dorman, J., Nakamura, Y., Ewing, M., 1974. Lunar seismicity, structure and tectonics. Reviews of Geophysics 12, 1.
Larose, E., Khan, A., Nakamura, Y., Campillo, M., 2005. Lunar subsurface investigated from correlation of seismic noise. Geophysical Research Letters 32. http://dx.doi.org/10.1029/2005GL023518.
Latham, G.V., Ewing, M., Press, F., Sutton, G., 1969. Apollo passive seismic experiment. Science 165, 241.
Latham, G.V., Ewing, M., Press, F., Sutton, G., Dorman, J.H., Nakamura, Y., Toksöz, M.N., Wiggins, R., Derr, J., Duennebier, F.K., 1970a. Passive seismic experiment. Science 167, 455.
Latham, G.V., Ewing, M., Dorman, J.H., Press, F., Toksöz, M.N., Sutton, G., Meissner, R., Duennebier, F.K., Nakamura, Y., Kovach, R., Yates, M., 1970b. Seismic data from man-made impacts on the Moon. Science 170, 620.
Latham, G.V., Ewing, M., Dorman, J.H., Lammlein, D., Press, F., Toksoz, M.N., Sutton, G., Duennebier, F.K., Nakamura, Y., 1971. Moonquakes. Science 174, 687.
Latham, G.V., Ewing, M., Press, F., Sutton, G., Dorman, J.H., Nakamura, Y., Toksöz, M.N., Lammlein, D., Duennebier, F.K., 1972. Passive seismic experiment. Apollo 16 Preliminary Science Report. NASA Spec. Publ. (NASA SP-315, sec. 9, 29 pp.).
Latham, G.V., Ewing, M., Dorman, J.H., Nakamura, Y., Press, F., Toksöz, M.N., Sutton, G., Duennebier, F.K., Lammlein, D., 1973. Lunar structure and dynamics—results from the Apollo passive seismic experiment. The Moon 7, 396.
Lemoine, F.G., Smith, D.E., Zuber, M.T., Neumann, G.A., Rowlands, D.D., 1997. A 70th degree lunar gravity model (GLGM-2) from Clementine and other tracking data. Journal of Geophysical Research 102, 16339.
Lognonné, P., 2005. Planetary seismology. Annual Review of Earth and Planetary Science 33, 571.
Lognonné, P., Johnson, C.L., 2007. Planetary seismology. Treatise in Geophysics, vol. 10 (ch. 4).
Lognonné, P., Gagnepain-Beyneix, J., Chenet, H., 2003. A new seismic model of the Moon: implications for structure, thermal evolution and formation of the Moon. Earth and Planetary Science Letters 211, 27.
Lognonné, P., Le Feuvre, M., Johnson, C.L., Weber, R.C., 2009. Moon meteoritic seismic hum: steady state prediction. Journal of Geophysical Research 114, E12003. http://dx.doi.org/10.1029/2008JE003294.
Longhi, J., 1980. A model of early lunar differentiation. Proceedings of Lunar and Planetary Science Conference, 11, pp. 289–315.
Longhi, J., 1982. Effects of fractional crystallization and cumulus processes on mineral composition trends of some lunar and terrestrial rock series. Lunar Planet. Sci. XIII. Lunar Planet. Inst., Houston, pp. 54–64.
Longhi, J., 2003. A new view of lunar anorthosites: postmagma ocean petrogenesis. Journal of Geophysical Research 108, 5083.
Longhi, J., 2006. Petrogenesis of picritic mare magmas: constraints on the extent of early lunar differentiation. Geochimica et Cosmochimica Acta 70, 5919–5934.
Lucey, P.G., Taylor, G.J., Malaret, E., 1995. Abundance and distribution of iron on the Moon. Science 268, 1150.

Lyubetskaya, T., Korenaga, J., 2007. Chemical composition of Earth's primitive mantle and its variance: 1. Method and results. Journal of Geophysical Research 112, B03211. http://dx.doi.org/10.1029/2005JB004223.
Margot, J.-L., Campbell, D.B., Jurgens, R.F., Slade, M.A., 1999. The topography of Tycho Crater. Journal of Geophysical Research 104 (11875), 1999.
Matsumoto, K., Goossens, S., Ishihara, Y., Liu, Q., Kikuchi, F., Iwata, T., Namiki, N., Noda, H., Hanada, H., Kawano, N., Lemoine, F.G., Rowlands, D.D., 2010. An improved lunar gravity field model from SELENE and historical tracking data: revealing the farside gravity features. Journal of Geophysical Research 115, E06007. http://dx.doi.org/10.1029/2009JE003499.
McDonough, W.F., Sun, S.S., 1995. The composition of the Earth. Chemical Geology 120 (3–4), 223.
Melosh, H.J., 1989. Impact Cratering: A Geologic Process. Oxford University Press, UK.
Mimoun, D., et al., 2011. Farside explorer: unique science from a mission to the farside of the moon. Experimental Astronomy. http://dx.doi.org/10.1007/s10686-011-9252-3.
Minshull, T.A., Goulty, N.R., 1988. The influence of tidal stresses on deep moonquake activity. Physics of the Earth and Planetary Interiors 52, 41.
Mueller, S., Taylor, G.J., Phillips, R.J., 1988. Lunar composition—a geophysical and petrological synthesis. Journal of Geophysical Research 93, 6338.
Nakamura, Y., 1977a. Seismic energy transmission in an intensely scattering environment. Journal of Geophysics 43, 389.
Nakamura, Y., 1977b. HFT events: shallow moonquakes? Physics of the Earth and Planetary Interiors 14, 217.
Nakamura, Y., 1978. A1 moonquakes: source distribution and mechanism. Proceedings of Lunar and Planetary Science Conference 9th, p. 3589.
Nakamura, Y., 1980. Shallow moonquakes: how they compare with earthquakes. Proceedings of Lunar and Planetary Science Conference 11th, p. 1847.
Nakamura, Y., 1983. Seismic velocity structure of the lunar mantle. Journal of Geophysical Research 88, 677.
Nakamura, Y., 2003. New identification of deep moonquakes in the Apollo lunar seismic data. Physics of the Earth and Planetary Interiors 139, 197.
Nakamura, Y., 2005. Farside deep moonquakes and deep interior of the Moon. Journal of Geophysical Research Planets 110. http://dx.doi.org/10.1029/2004JE002332.
Nakamura, Y., 2010. Lunar seismology: current status and future challenges. Deutsche Geophysikalische Gesellschaft Mitteilungen V (3), 4.
Nakamura, Y., 2011. Timing problem with the Lunar Module impact data as recorded by LSPE and corrected near-surface structure at the Apollo 17 landing site. Journal of Geophysical Research 116. http://dx.doi.org/10.1029/2011JE003972.
Nakamura, Y., Koyama, J., 1982. Seismic Q of the lunar upper mantle. Journal of Geophysical Research Planets 87, 4855.
Nakamura, Y., Lammlein, D., Latham, G., Ewing, M., Dorman, J., Press, F., Toksoz, M., 1973. New seismic data on the state of the deep lunar interior. Science 181, 49.
Nakamura, Y., Latham, G., Lammlein, D., Ewing, M., Duennebier, F., Dorman, J., 1974a. Deep lunar interior inferred from recent seismic data. Geophysical Research Letters 1, 137.
Nakamura, Y., Dorman, J., Duennebier, R., Ewing, M., Lammlein, D., Latham, G., 1974b. High-frequency lunar teleseismic events. Proceedings of Lunar and Planetary Science Conference 5th, p. 2883.
Nakamura, Y., Dorman, J.H., Duennebier, F.K., Lammlein, D., Latham, G.V., 1975. Shallow lunar structure determined from the passive seismic experiment. Moon 13, 57.
Nakamura, Y., Latham, G., Dorman, H., Ibrahim, A., Koyama, J., Horvath, P., 1979. Shallow moonquakes: depth, distribution and implications as to the present state of the lunar interior. Proceedings of Lunar and Planetary Science Conference 10th, p. 2299.
Nakamura, Y., Latham, G., Dorman, J., 1980. How we processed Apollo lunar seismic data. Physics of the Earth Planetary Interiors 21, 218.
Nakamura, Y., Latham, G., Dorman, J., Harris, J., 1981. Passive seismic experiment long-period event catalog, Final Version, 1969 day 202–1977 day 273. Galveston Geophysical Laboratory Contribution, 491. Univ. of Tex., Austin (314 pp.).
Nakamura, Y., Latham, G., Dorman, J., 1982. Apollo Lunar Seismic Experiment—final summary. Journal of Geophysical Research 87 (A117), 1982.
Namiki, N., et al., 2009. Farside gravity field of the Moon from four-way Doppler measurements of SELENE (Kaguya). Science 323, 900. http://dx.doi.org/10.1126/science.1168029.
Namur, O., Charlier, B., Pirard, C., Hermann, J., Liégeois, J.-P., Vander Auwera, J., 2011. Anorthosite formation by plagioclase flotation in ferrobasalt and implications for the lunar crust. Geochimica et Cosmochimica Acta 75, 4998–5018.
Neal, C.R., 2001. Interior of the Moon: the presence of garnet in the primitive deep lunar mantle. Journal of Geophysical Research 106, 27865.
Neal, C.R., 2009. The Moon 35 years after Apollo: what's left to learn? Chemie der Erde-Geochemistry 69, 3. http://dx.doi.org/10.1016/j.chemer.2008.07.002.
Neumann, G.A., Zuber, M.T., Smith, D.E., Lemoine, F.G., 1996. The lunar crust: global structure and signature of major basins. Journal of Geophysical Research 101 (16841), 1996.
Nimmo, F., Faul, U.H., Garnero, E.J., 2012. Dissipation at tidal and seismic frequencies in a melt-free Moon. Journal of Geophysical Research 117, E09005. http://dx.doi.org/10.1029/2012JEE004160.
Nozette, S., et al., 1994. The clementine mission to the moon: Scientific overview. Science 266 (5192), 1835–1839. http://dx.doi.org/10.1126/science.266.5192.1835.
O'Neill, H.S., 1991. The origin of the Moon and the early history of the Earth: a chemical model. Part 1: The Moon. Geochimica et Cosmochimica Acta 55, 1135–1157.
Oberst, J., Nakamura, Y., 1991. A search for clustering among the meteoroid impacts detected by the Apollo lunar seismic network. Icarus 91, 315.
Ohtake, M., et al., 2009. The global distribution of pure anorthosite on the Moon. Nature 461, 236–240.
Pahlevan, K., Stevenson, D.J., Eiler, J.M., 2011. Chemical fractionation in the silicate vapor atmosphere of the Earth. Earth and Planetary Science Letters 301. http://dx.doi.org/10.1016/j.epsl.2010.10.036.
Palme, H., Nickel, K.G., 1985. Ca/Al ratio and composition of the Earth's upper mantle. Geochemica Cosmochima Acta 49, 2123.
Palme, H., Spettel, B., Jochum, K.F., et al., 1991. Lunar highland meteorites and the composition of the lunar crust. Geochimica et Cosmochimica Acta 55, 3105.
Ping, J.S., Heki, K., Matsumoto, K., et al., 2003. A degree 180 spherical harmonic model for the lunar topography. Advances in Space Research 31 (11), 2377–2382.
Prettyman, T.H., Feldman, W.C., Lawrence, D.J., McKinney, G.W., Binder, A.B., Elphic, R.C., Gasnault, O.M., Maurice, S., Moore, K.R., 2002. Library least squares analysis of Lunar Prospector gamma ray spectra, Lunar and Planetary Science XXXIII, abstract 2012. Lunar and Planetary Institute, Houston.
Pullan, S., Lambeck, K., 1980. On constraining lunar mantle temperatures from gravity data. Proc. Lunar Planet. Sci. Conf., 11th, p. 2031.
Righter, K., 2002. Does the Moon have a metallic core? Constraints from giant-impact modelling and siderophile elements. Icarus 158, 1.
Ringwood, A.E., 1966. Mineralogy of the mantle. In: Hurley, P. (Ed.), Advances in Earth Science. MIT Press, Cambridge, Mass, p. 357.
Ringwood, A.E., 1977. Basaltic magmatism and bulk composition of Moon. 1. Major and heat-producing elements. Moon 16, 389.
Ringwood, A.E., 1979. Origin of the Earth and Moon. Springer, New York.
Ryder, G., Spudis, P.D., 1987. Chemical composition and origin of Apollo 15 impact melts. Proceedings of Lunar Planet Science Conference 17th: Journal of Geophysical Research, 92, p. E432.
Saal, A.E., Hauri, E.H., Cascio, M.L., van Orman, J.A., Rutherford, M.C., Cooper, R.F., 2008. Volatile content of lunar volcanic glasses and the presence of water in the Moon's interior. Nature 454. http://dx.doi.org/10.1038/nature07047.
Sabra, K.G., Gerstoft, P., Roux, P., Kuperman, W.A., Fehler, M.C., 2005. Surface-wave tomography from microseisms in Southern California. Geophysical Research Letters 32, L14311. http://dx.doi.org/10.1029/2005GL023155.
Sakamaki, T., Ohtani, E., Urakawa, S., Suzuki, A., Katayama, Y., Zhao, D., 2010. Density of high-Ti basalt magma at high pressure and origin of heterogeneities in the lunar mantle. Earth and Planetary Science Letters 299. http://dx.doi.org/10.1016/j.epsl.2010.09.007.
Salters, V.J.M., Stracke, A., 2004. Composition of the depleted mantle. Geochemistry, Geophysics, Geosystems 5, Q05B07. http://dx.doi.org/10.1029/2003GC000597.
Scholten, F., Oberst, J., Matz, K.-D., Roatsch, T., Whlisch, M., Speyerer, E.J., Robinson, M.S., 2012. GLD100: the near-global lunar 100 m raster DTM from LROC WAC stereo image data. Journal of Geophysical Research 117, E3. http://dx.doi.org/10.1029/2011JE003926.
Schreiber, E., Anderson, O.L., 1970. Properties and composition of lunar materials: Earth analogies. Science 168, 1579.
Sellers, P., 1992. Seismic evidence for a low-velocity lunar core. Journal of Geophysical Research 97, 11663.
Sens-Schönfelder, C., Larose, E., 2008. Temporal changes in the lunar soil from correlation of diffuse vibrations. Physical Review E 78 (045601(R)).
Shapiro, N.M., Campillo, M., 2004. Emergence of broadband Rayleigh waves from correlations of the ambient seismic noise. Geophysical Research Letters 31, L07614. http://dx.doi.org/10.1029/2004GL019491.
Shearer, C.K., Papike, J.J., 1999. Magmatic evolution of the Moon. American Mineralogist 84, 1469–1494.
Shearer, C.K., Papike, J.J., Galbreath, K.C., Shimizu, N., 1991. Exploring the lunar mantle with secondary ion mass spectrometry: a comparison of lunar picritic glass beads from the Apollo 14 and Apollo 17 sites. Earth and Planetary Science Letters 102, 134–147.
Shearer, C.K., Papike, J.J., Layne, G.D., 1996. The role of ilmenite in the source region for mare basalts: evidence from niobium, zirconium, and cerium in picritic glasses. Geochimica et Cosmochimica Acta 60, 3521–3530.
Shearer, C.K., Hess, P.C., Wieczorek, M.A., Pritchard, M.E., Parmentier, E.M., Borg, L.E., Longhi, J., Elkins-Tanton, L.T., Neal, C.R., Antonenko, I., Canup, R.M., Halliday, A.N., Grove, T.L., Hager, B.H., Lee, D.-C., Wiechert, U., 2006. Thermal and magmatic evolution of the Moon. In: Jolliff, B.L., Wieczorek, M.A., Shearer, C.K., Neal, C.R. (Eds.), New views of the Moon: Reviews in Mineralogy and Geochemistry, vol. 60, p. 365.
Simmons, G., Siegfried, R., Richter, D., 1975. Characteristics of microcracks in lunar samples. Proceedings of Lunar Science Conference 6th, p. 3227.
Smith, J.V., Anderson, A.T., Newton, R.C., Olsen, E.J., Wyllie, P.J., Crewe, A.V., Isaacson, M.S., Johnson, D., 1970. Petrologic history of the Moon inferred from petrography, mineralogy, and petrogenesis of Apollo 11 rocks. Proceedings of the Apollo 11 Lunar Science Conference. Pergamon Press, pp. 897–925.
Smith, D.E., Zuber, M.T., Neumann, G.A., Lemoine, F.G., 1997. Topography of the Moon from the Clementine lidar. Journal of Geophysical Research 102, 1591.
Smith, D.E., et al., 2010. The lunar orbiter laser altimeter investigation on the lunar reconnaissance orbiter mission. Space Science Reviews 150, 209. http://dx.doi.org/10.1007/s11214-009-9512-y.
Snyder, G.A., Taylor, L.A., Neal, C.R., 1992. A chemical model for generating the sources of mare basalts: combined equilibrium and fractional crystallization of the lunar magma-sphere. Geochimica et Cosmochimica Acta 56, 3809–3823.
Solomon, S.C., Chaiken, J., 1976. Thermal expansion and thermal stress in the Moon and terrestrial planets: clues to early thermal history. Proceedings of Lunar Science Conference 7th, p. 3229.
Sonnett, C.P., 1982. Electromagnetic induction in the Moon. Reviews of Geophysics and Space Physics 20, 411.
Spera, F.J., 1992. Lunar magma transport phenomena. Geochimica et Cosmochimica Acta 56, 2253–2265.
Spudis, P., Hawke, B.R., Lucey, P., 1984. Composition of Orientale basin deposits and implications for the lunar basin-forming process. Proc. Lunar Planet. Sci. Conf. 15th, Part 1Journal of Geophysical Research 89, C197 (Suppl.).
Steinhart, J., 1967. Mohorovicic discontinuity. In: Runcorn, S. (Ed.), International Dictionary of Geophysics. Pergamon Press, p. 991.

Tanimoto, T., Eitzel, M., Yano, T., 2008. The noise cross-correlation approach for Apollo 17 LSPE data: diurnal change in seismic parameters in shallow lunar crust. Journal of Geophysical Research 113. http://dx.doi.org/10.1029/2007JE003016.
Tarantola, A., 2005. Inverse Problem Theory and Methods for Model Parameter Estimation. SIAM, Philadelphia, USA.
Taylor, S.R., 1980. Refractory and moderately volatile element abundances in the Earth, Moon and meteorites. Proc. Lunar Planet. Sci. Conf. 11th, p. 333.
Taylor, S.R., 1982. Planetary science: a lunar perspective. Lunar and Planetary Institute, Houston, TX, p. 481.
Taylor, S.R., 1986. The origin of the Moon: geochemical considerations. In: Hartmann, W.K., Phillips, R.J., Taylor, G.J. (Eds.), Origin of the Moon. Lunar Planet. Inst., Houston, Tex., p. 125.
Taylor, S.R., Jakes, P., 1974. The geochemical evolution of the Moon. Proc. Lunar Sci. Conf. 5th, p. 1287.
Taylor, S.R., Taylor, G.J., Taylor, L.A., 2006. The Moon: a Taylor perspective. Geochimica et Cosmochimica Acta 70, 5904.
Thacker, C., Liang, Y., Peng, Q., Hess, P.C., 2009. The stability and major element partitioning of ilmenite and armalcolite during lunar cumulate mantle overturn. Geochimica et Cosmochimica Acta 73, 820–836.
Todd, T., Richter, D.A., Simmons, G., Wang, H., 1973. Unique characterization of lunar samples by physical properties. Proceedings of Lunar Science Conference 4th, p. 2639.
Toksöz, M.N., Press, F., Anderson, K., Dainty, A., Latham, G., Ewing, M., Dorman, J., Lammlein, D., Nakamura, Y., Sutton, G., Duennebier, F., 1972. Velocity structure and properties of the lunar crust. Moon 4, 490.
Toksöz, M.N., Dainty, A.M., Solomon, S.C., Anderson, K., 1974. Structure of the Moon. Reviews of Geophysics 12, 539.
Toksöz, M.N., Goins, N.R., Cheng, H.C., 1977. Moonquakes: mechanisms and relations to tidal stresses. Science 196, 929.
Tompkins, S., Pieters, C.M., 1999. Mineralogy of the lunar crust: results from Clementine. Meteorits and Planetary Science 34, 25.
Tonks, W.B., Melosh, H.J., 1990. The physics of crystal settling and suspension in a turbulent magma ocean. In: Newsom, H.E., Jones, J.H. (Eds.), Origin of the Earth. Oxford University Press, p. 151.
van Kan Parker, M., Sanloup, C., Sator, N., Guillot, B., Tronche, E.J., Perrillat, J.-P., Mezouar, M., Rai, N., van Westrenen, W., 2012. Neutral buoyancy of titanium-rich melts in the deep lunar interior. Nature Geoscience 5. http://dx.doi.org/10.1038/ngeo1402.
Vinnik, L., Chenet, H., Gagnepain-Beyneix, J., Lognonné, P., 2001. First seismic receiver functions on the Moon. Geophysical Research Letters 28, 3031.
Wänke, H., Dreibus, G., 1986. Geochemical evidence for the formation of the Moon by impact-induced fission of the proto-Earth. In: Hartmann, W.K., Phillips, R.J., Taylor, G.J. (Eds.), Origin of the Moon. Lunar and Planetary Institute, Houston, TX, p. 649.
Warren, P.H., 1985. The magma ocean concept and lunar evolution. Annual Review of Earth Planetary Science 13, 201.
Warren, P.H., 1986. The bulk-Moon MgO/FeO ratio: a highlands perspective. In: Hartmann, W.K., Phillips, R.J., Taylor, G.J. (Eds.), Origin of the Moon. Lunar Planet. Inst., Houston, Tex., p. 279.
Warren, P.H., 1990. Lunar anorthosites and the magma-ocean plagioclase-flotation hypothesis: importance of FeO enrichment in the parent magma. American Mineralogist 75, 46–58.
Warren, P.H., 2005. "New" lunar meteorites: implications for composition of the global lunar surface, lunar crust, and the bulk Moon. Meteoritics and Planetary Science 40, 477–506.
Warren, P.H., Rasmussen, K.L., 1987. Megaregolith insulation, internal temperatures, and bulk uranium content of the Moon. Journal of Geophysical Research 92, 3453.
Weber, R.C., Bills, B.G., Johnson, C.L., 2009. Constraints on deep moonquake focal mechanisms through analyses of tidal stress. Journal of Geophysical Research 114 (E050010.1029/2008JE003286).
Weber, R.C., Lin, P.-Y., Garnero, E.J., Williams, Q., Lognonné, P., 2010. Seismic detection of the lunar core. Science. http://dx.doi.org/10.1126/science.1199375.
Wieczorek, M.A., 2003. The thickness of the lunar crust: how low can you go? Lunar and Planetary Science XXXIV (abstract 1330 (CD-ROM)).
Wieczorek, M.A., Phillips, R.J., 1998. Potential anomalies on a sphere: applications to the thickness of the lunar crust. Journal of Geophysical Research 103, 1715–1724. http://dx.doi.org/10.1029/97JE03136.
Wieczorek, M.A., Phillips, R.J., 2000. The Procellarum KREEP Terrane: implications for mare volcanism and lunar evolution. Journal of Geophysical Research 105, 20417.
Wieczorek, M.A., Zuber, M.T., 2001. The composition and origin of the lunar crust: constraints from central peaks and crustal thickness modeling. Geophysical Research Letters 28, 4023.
Wieczorek, M.A., Joliff, B.L., Khan, A., Pritchard, M.E., Weiss, B.P., Williams, J.G., Hood, L.L., Righter, K., Neal, C.R., Shearer, C.K., McCallum, I.S., Tompkins, S., Hawke, B.R., Peterson, C., Gillis, J.J., Bussey, B., 2006. The constitution and structure of the lunar interior. Reviews in Mineralogy and Geochemistry 60, 221. http://dx.doi.org/10.2138/rmg.2006.60.3.
Wieczorek, M.A., et al., 2013. The crust of the moon as seen by GRAIL. Science 339, 671–675. http://dx.doi.org/10.1126/science.1231530.
Williams, J.G., Boggs, D.H., Yoder, C.F., Radcliff, J.T., Dickey, J.O., 2001. Lunar rotational dissipation in solid body and molten core. Journal of Geophysical Research 106, 27933.
Williams, J.G., Boggs, D.H., Ratcliff, J.T., 2012. Lunar moment of inertia, Love number and core. Lunar and Planetary Science Conference XLIII, abstract 2230. Lunar and Planetary Institute, Houston.
Wiskerchen, M.J., Sonett, C.P., 1977. A lunar metal core? Proceedings of Lunar and Planetary Science Conference 8th, p. 515.
Wood, J.A., 1986. Moon over Mauna Lea: a review of hypotheses of formation of Earth's Moon. In: Hartman, W.K., Philipps, R.J., Taylor, G.J. (Eds.), Origins of the Moon. Lunar and Planetary Institute, Houston, pp. 17–55.
Wood, J.A., Dickey, J.S., Marvin, U.B., Powell, B.N., 1970. Lunar anorthosites and a geophysical model of the Moon. Proceedings of the Apollo 11 Lunar Science Conference. Pergamon Press, p. 965.
Yamada, H., Garcia, R.F., Lognonné, P., Le Feuvre, M., Calvet, M., Gagnepain-Beyneix, J., 2011. Optimisation of seismic network design: application to a geophysical international lunar network. Planning Space Sciences 59, 343. http://dx.doi.org/10.1016/j.pss.2010.12.007.
Zhao, D., Lei, J., Liu, L., 2008. Seismic tomography of the Moon. Chinese Science Bulletin 53, 3897. http://dx.doi.org/10.1007/s11434-008-0484-1.
Zuber, M.T., Smith, D.E., Lemoine, F.G., Neumann, G.A., 1994. The shape and internal structure of the Moon from the Clementine mission. Science 266, 1839.
Zuber, M.T., et al., 2012. Constraints on the volatile distribution within Shackleton crater at the lunar south pole. Nature 486, 378. http://dx.doi.org/10.1038/nature11216.
Zuber, M.T., Smith, D.E., Lehman, D.H., Hoffman, T.L., Asmar, S.W., Watkins, M.M., 2013a. Gravity Recovery and Interior Laboratory (GRAIL): mapping the lunar interior from crust to core. Space Science Reviews. http://dx.doi.org/10.1007/s11214-012-9952-7 (online).
Zuber, M.T., et al., 2013b. Gravity field of the moon from the gravity recovery and interior laboratory (GRAIL) Mission. Science 339, 668. http://dx.doi.org/10.1126/science.1231507.